Electronic Supplementary Information

Macrocyclic *C*,*C*′-Diaryl-*o*-Carborane Derivatives Containing Pseudo-Crown Ether: Emission Enhancement upon Cation Recognition

Mei Tokutomi,[a] Kazuhiro Yuhara,[a] Kazuo Tanaka*[a,b]

[a] Department of Polymer Chemistry, Graduate School of Engineering, Kyoto University, Katsura, Nishikyo-ku, Kyoto 615–8510, Japan

[b] Department of Technology and Ecology, Graduate School of Global Environmental Studies, Kyoto University, Katsura, Nishikyo-ku, Kyoto 615-8510, Japan

E-mail: tanaka@poly.synchem.kyoto-u.ac.jp

Index

General

NMR spectroscopy

^{1}H (400 or 600 MHz), ^{13}C{^{1}H} (100 or 150 MHz), and ^{11}B{^{1}H} (128 MHz) NMR spectra were recorded on JEOL JNM-ECZ 400, JEOL JNM-ECZ 400S, and/or JEOL JNM-ECZ 600R spectrometers. The ^{1}H and ^{13}C{^{1}H} NMR chemical shift values were expressed relative to tetramethylsilane (0.00 ppm) and/or residual non-deuterated solvent peaks (5.32 ppm for $CDHCl_2$ in CD_2Cl_2, 7.26 ppm for $CHCl_3$ in $CDCl_3$) were used as internal standards. The ^{11}B{^{1}H} chemical shift values were expressed relative to $BF_3{\cdot}Et_2O$ (0.00 ppm) as an external standard.

High-resolution mass spectrometry (HRMS)

HRMS spectrometry was performed at the Technical Support Office (Department of Synthetic Chemistry and Biological Chemistry, Graduate School of Engineering, Kyoto University) and HRMS were obtained on a Thermo Fisher Scientific EXACTIVE spectrometer for electron spray ionization (ESI) or atmospheric pressure chemical ionization (APCI).

Optical measurements

UV–vis absorption spectra were obtained on a SHIMADZU UV3600i Plus spectrophotometer. Photoluminescence spectra were obtained on a Horiba FluoroLog-3 luminescence spectrometer. Absolute photoluminescence quantum yield values were measured with a Hamamatsu Photonics Quantaurus-QY Plus C13534-01 model. Photoluminescence lifetimes were measured by a DeltaFlex spectrofluorometer system with DeltaDiode UV diode laser (375 nm). Temperature control of UV-vis absorption and photoluminescence measurement were performed with an Oxford Optistat DN temperature controller.

Relative quantum yield ($\Phi_{PL,rel}$) was calculated by the following equation[1]

$$\Phi_{PL,rel} = \Phi_s \times \left(\frac{A_s}{A_x}\right) \times \left(\frac{F_x}{F_s}\right) \times \left(\frac{n_x}{n_s}\right)^2$$

,where Φ_S, A, F, and n were quantum yield of the standard, absorption, integrated emission intensities, and refractive index, respectively. The x subscript refers to the unknown and s refers to the reference. A $CHCl_3$ solution (1.0×10^{-5} M) of $Ru(bpy)_3Cl_2{\cdot}6H_2O$ was used as a reference.

Single-crystal X-ray diffraction analysis

X-ray crystallographic analysis was carried out by a Rigaku Saturn 724+ with MicroMax-007 HF CCD diffractometer with Varimax Mo optics using graphite-monochromated Mo$K\alpha$ radiation. The structures were solved with SHELXT 2015[2] and refined on F^2 with SHELXL 2015[3] on Olex 2-1.5.[4] All hydrogen atoms were placed at calculated positions and refined using a riding model. The

program Mercury 2023.3.0[5] was used to generate the X-ray structural diagram.

Powder X-ray diffraction (PXRD) analysis

PXRD data were collected with a Rigaku SmartLab Diffractometer (sealed tube (50 kV, 40 mA); Cu Kα, 1.542 Å; Bragg–Brentano geometry). PXRD samples were placed on a single-crystal silicon substrate.

Computational methods

The Gaussian16 Rev.C.01 program package[6] was used for structural optimization. First, optimized structures of isolated molecules in the ground S_0 states and their electric structures were calculated. The density functional theory (DFT) was applied for the optimization of the structures in the S_0 states at B3PW91-D3/6-31+G(d,p) level. The optimized geometry was confirmed to be the local minima by performing frequency calculations and obtaining only positive frequencies.

Synthetic Equipment

Column chromatography was performed with Wakogel C-300 silica gel. Analytical thin-layer chromatography (TLC) was performed with silica gel 60 Merck F_{254} plates.

Materials

Commercially available compounds used without purification

Tetrakis(triphenylphosphine)palladium(0) ($Pd(PPh_3)_4$) (Tokyo Chemical Industry Co., Ltd.)

KPF_6 (Fujifilm Wako Pure Chemical Corporation)

Na_2CO_3 (Fujifilm Wako Pure Chemical Corporation)

K_2CO_3 (Fujifilm Wako Pure Chemical Corporation)

4-(4,4,5,5-Tetramethyl-1,3,2-dioxaborolan-2-yl)anisole (**Bpin-Ph-OMe**) (Tokyo Chemical Industry Co., Ltd.)

4-Bromobenzyl bromide (Tokyo Chemical Industry Co., Ltd.)

Sodium benzenesulfinate dihydrate (Tokyo Chemical Industry Co., Ltd.)

9,10-Dibromoanthracene (Fujifilm Wako Pure Chemical Corporation)

n-Butyllithium, in *n*-Hexane (Kanto Chemical Co., Inc.)

Diethyl chlorophosphate (Tokyo Chemical Industry Co., Ltd.)

Lithium bis(trimethylsilyl)amide (ca. 26% in Tetrahydrofuran, ca. 1.3 mol/L) (Tokyo Chemical Industry Co., Ltd.)

Decaborane ($B_{10}H_{14}$) (Toronto Research Chemicals)

Silver nitrate (Fujifilm Wako Pure Chemical Corporation)

Tetraethylene glycol bis(*p*-toluenesulfonate) (Tokyo Chemical Industry Co., Ltd.)

4-(4,4,5,5-Tetramethyl-1,3,2-dioxaborolan-2-yl)phenol (Fujifilm Wako Pure Chemical Corporation)
Rubidium chloride (Wako Pure Chemical Corporation)
Cesium chloride (Fujifilm Wako Pure Chemical Corporation)
Tris(2,2'-bipyridyl)ruthenium(II) chloride hexahydrate (Tokyo Chemical Industry Co., Ltd.)

Commercially available solvent used after purification

Tetrahydrofuran (THF) was purified using a two-column solid-state purification system (Glasscontour System, Joerg Meyer, Irvine, CA).

Commercially available solvents

N, N-Dimethylformamide, Deoxidized (Fujifilm Wako Pure Chemical Corporation)
Toluene, Deoxidized (Fujifilm Wako Pure Chemical Corporation)
MeCN, Super Dehydrated (Fujifilm Wako Pure Chemical Corporation)
$CDCl_3$ (Eurisotop)
CD_2Cl_2 (Eurisotop)
Acetone-d_6 (Tokyo Chemical Industry Co., Ltd.)

Compounds prepared and characterized as described in the literatures

Br1[7] (4 steps, 18% overall yield from 4-Bromobenzyl bromide (1 step, 29% yield from 9-Bromo-10-[2-(4-bromophenyl)ethynyl]anthracene))
Br2[8] (1 step, 27% overall yield from 1,2-Bis(4-bromophenyl)ethyne)
Bpin-Ph-TEG[9] (1 step, 58% yield from 4-(4,4,5,5-Tetramethyl-1,3,2-dioxaborolan-2-yl)phenol)
$RbPF_6$[10] (1 step, 33% yield from Ammonium hexafluorophosphate)
$CsPF_6$[10] (1 step, 63% yield from Ammonium hexafluorophosphate)

NMR titration

NMR titration was conducted by using the modified procedures according to the literature.[11] ^{1}H NMR titration experiments were performed on JEOL JNM-ECZ 400 and JEOL JNM-ECZ 400S spectrometer. In this experiment, a solution of hexafluorophosphate salt (potassium, rubidium, and cesium) in acetone-d_6 was added to a solution of macrocycle in $CDCl_3$ at 298 K.

A 40.0 mM solution of the salt was added to 200 μL of a 5.0 mM solution of macrocycle, where 1.0 equivalent of salt added corresponds to 25.0 μL of the salt solution. As for titration of cesium hexafluorophosphate and **C2**, 10.0 mM of the salt was prepared and added in addition of 40.0 mM salt solution. All titration was performed in the mixed solvent of acetone-d_6/$CDCl_3$ 3/2(v/v). Association constants were estimated by using the non-linear fitting tool provided by the open access web portal Supramolecular.org (http://supramolecular.org).

Job plot

The stoichiometry of the interaction of macrocycles and cations was determined by Job's method based on the chemical shift change (δ) of the TEG protons (H4 for **C1** and H1 for **C2**) and the molar fraction of **C1** or **C2** (χ). All titration was performed in the mixed solvent of acetone-d_6/$CDCl_3$ (3/2, v/v). [**C1** or **C2**] + [MPF_6] = 4 mM.

Synthetic Procedures

Synthesis of C1

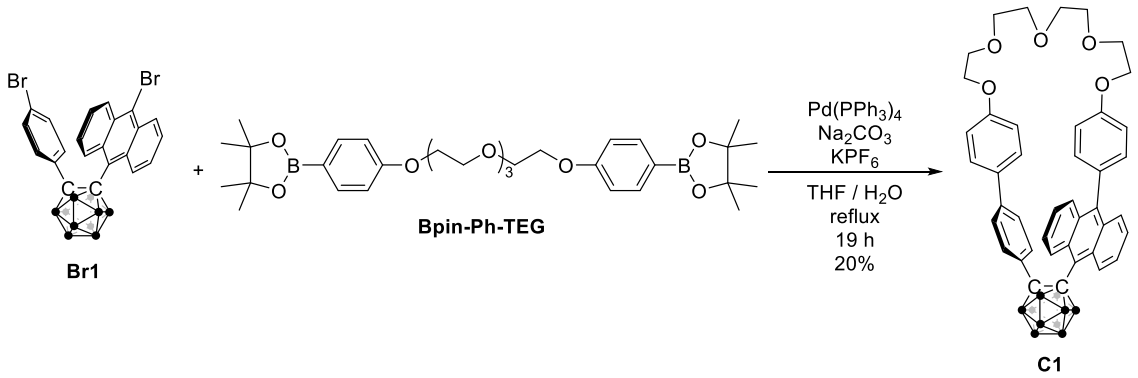

Scheme S1. Synthetic scheme of **C1**.

Bpin-Ph-TEG (0.326 g, 0.55 mmol) and THF (4.0 mL) was added and stirred at room temperature under N_2 atmosphere. To a 1 L 2-necked round-bottom flask, THF (ca. 700 mL), **1** (0.279 g, 0.50 mmol), KPF_6 (0.466 g, 2.53 mmol), Na_2CO_3 (0.275 g, 2.60 mmol), $Pd(PPh_3)_4$ (0.017 g, 0.014 mmol), **Bpin-Ph-TEG** solution in THF, and H_2O (125 mL) were added under N_2 atmosphere. The mixture was refluxed for 15 h under N_2 atmosphere. After cooling to room temperature, the solvent was evaporated with a rotary evaporator. The mixture was extracted with CH_2Cl_2. The organic layer was washed with brine and dried over $MgSO_4$. After filtration and evaporation of the solvent to afford orange solid, the crude was supported by silica in $CHCl_3$ and purified by silica gel column chromatography (eluent: AcOEt/ *n*-hexane = 2/1(v/v)). Recrystallization from MeOH afforded orange powder (0.068 g, 0.09 mmol, 20%).

^{1}H NMR (600 MHz, $CDCl_3$ at 0 ºC): δ (ppm) = 9.03 (d, J = 9.0 Hz, 2H), 7.47 (ddd, J = 7.5, 1.8, 1.2 Hz, 2H), 7.35 (dd, J = 8.7, 0.9 Hz, 2H), 7.33 (d, J = 9.0, 2H), 7.24 (dd, J = 6.6, 0.6 Hz, 1H), 7.22 (dd, J = 6.6, 0.6 Hz, 1H), 7.19 (dd, J = 8.1, 1.5 Hz, 1H). 7.01 (d, J = 8.4, 2H), 6.97 (dd, J = 8.1, 2.1 Hz, 1H), 6.85 (d, J = 9.0 Hz, 2H), 6.54 (d, J = 8.4 Hz, 2H), 6.15 (dd, J = 8.4, 2.4 Hz, 1H), 6.01 (dd, J = 7.2, 1.2 Hz, 1H), 4.20 (t, J = 4.5 Hz, 2H), 4.05 (m, 2H), 3.97 (m, 2H), 3.94 (m, 2H) 3.79 (m, 4H), 3.76 (m, 4H), 4.2–2.0 (br, 10H).

^{13}C{^{1}H} NMR (150 MHz, $CDCl_3$ at 0 ºC): δ (ppm) = 159.1, 158.2, 142.8, 141.6, 133.4, 132.2, 131.3, 131.1, 130.8, 130.5, 129.6, 128.9, 128.1, 126.6, 126.3, 124.9, 124.8, 124.5, 118.6, 114.9, 114.3, 113.6, 95.6, 92.0, 71.1, 70.8, 70.6, 70.2, 69.5, 69.4, 67.9, 67.2.

Note: Due to the high rotational barrier of the phenyl ring on the anthracene unit, the atoms at inside and outside of the macrocycle were magnetically inequivalent.

^{11}B{^{1}H} NMR (128 MHz, $CDCl_3$): δ (ppm) = 0.36 (2B), −2.02 (2B), −9.25 (6B).

HRMS (ESI) calcd. for $C_{42}H_{46}B_{10}O_5K_1$ $[M+K]^+$ 779.3934, found 779.3977.

Synthesis of M1

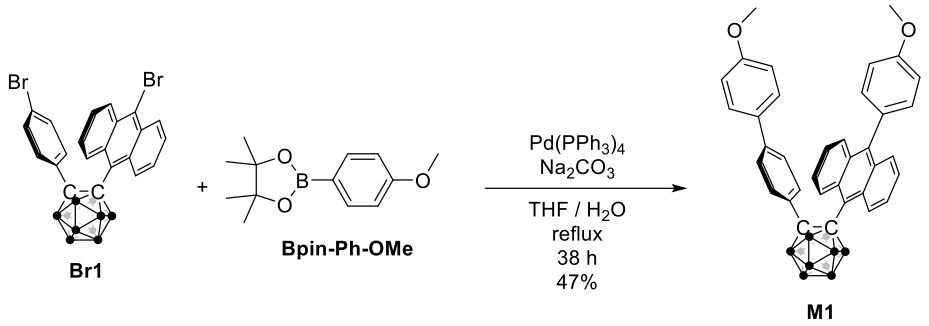

Scheme S2. Synthetic scheme of **M1**.

To a 100 mL 2-necked round-bottom flask, **Br1** (0.166 g, 0.30 mmol), **Bpin-Ph-OMe** (0.223 g, 0.90 mmol), Na_2CO_3 (0.085 g, 0.75 mmol), and $Pd(PPh_3)_4$ (0.013 g, 0.0068 mmol) were added under N_2 atmosphere. Then, THF (4.8 mL) and H_2O (0.8 mL) were added and refluxed for 38 h. After cooling to room temperature, the mixture was extracted with AcOEt. The organic layer was washed with brine and dried over $MgSO_4$. After filtration and evaporation of the solvent to afford orange solid, the crude was supported by silica in $CHCl_3$ and purified by silica gel chromatography (eluent: AcOEt/ *n*-hexane = 1/5(v/v)). Recrystallization from MeOH/$CHCl_3$ afforded deep orange powder (0.085 g, 0.14 mmol, 47%).

^{1}H NMR (600 MHz, $CDCl_3$ at 0 ºC): δ (ppm) = 9.06 (d, J = 9.0 Hz, 2H), 7.48 (ddd, J = 9.0, 6.6, 1.2 Hz, 2H), 7.37 (dd, J = 9.0, 1.2 Hz, 2H), 7.32 (d, J = 9.0 Hz, 2H), 7.24 (dd, J =5.7, 0.6 Hz, 1H), 7.23 (dd, J = 6.6, 0.6 Hz, 1H), 7.21 (d, J = 8.4 Hz, 1H), 7.00 (d, J = 6.6 Hz, 1H), 6.96 (d, J = 9.0 Hz, 2H), 6.84 (d, J = 8.4 Hz, 2H), 6.56 (d, J = 9.0 Hz, 2H), 6.38 (d, J = 7.2 Hz, 1H), 6.18 (d, J = 7.8 Hz, 1H), 3.87 (s, 3H), 3.83 (s, 3H), 4.0–1.8 (br, 10H).

^{13}C{^{1}H} NMR (150 MHz, $CDCl_3$ at 0 ºC): δ (ppm) = 159.6, 158.8, 142.6, 141.7, 133.3, 131.8, 131.5, 131.2, 130.6, 130.4, 129.6, 128.7, 128.1, 126.6, 126.3, 125.0, 124.9, 124.4, 118.5, 114.1, 113.7, 113.0, 95.2, 91.5, 55.4, 55.2.

Note: Due to the high rotational barrier of the phenyl ring on the anthracene unit, the atoms that face other phenyl group side and those that do not were magnetically inequivalent.

^{11}B{^{1}H} NMR (128 MHz, $CDCl_3$): δ (ppm) = 0.48 (1B), −1.95 (1B), −9.63 (8B).

HRMS (APCI) calcd. for $C_{36}H_{37}B_{10}O_2$ $[M+H]^+$ 609.3791, found 609.3807.

Synthesis of C2

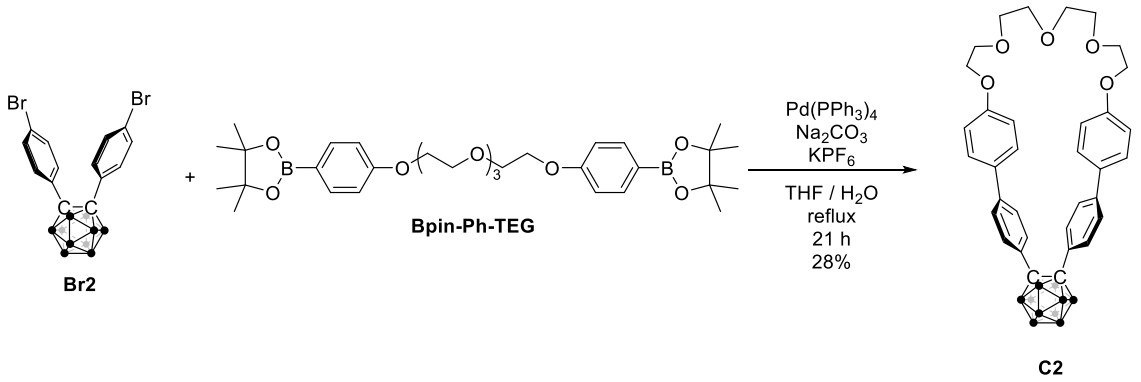

Scheme S3. Synthetic scheme of **C2**.

Bpin-Ph-TEG (0.474 g, 0.79 mmol) and THF (4.0 mL) was added and stirred at room temperature under N_2 atmosphere. To a 1 L 2-necked round-bottom flask, THF (ca. 700 mL), **Br2** (0.316 g, 0.70 mmol), KPF_6 (0.647 g, 3.50 mmol), Na_2CO_3 (0.381 g, 3.60 mmol), $Pd(PPh_3)_4$ (0.020 g, 0.017 mmol), **Bpin-Ph-TEG** solution in THF, and H_2O (100 mL) were added under N_2 atmosphere. The mixture was refluxed for 21 h under N_2 atmosphere. After cooling to room temperature, the solvent was evaporated with a rotary evaporator. The mixture was extracted with CH_2Cl_2. The organic layer was washed with brine and dried over $MgSO_4$. After filtration and evaporation of the solvent to afford brown solid, the crude was supported by silica in $CHCl_3$ and purified by silica gel column chromatography (eluent: AcOEt/*n*-hexane = 2/1(v/v)). Recrystallization from MeOH and decantation from *n*-hexane afforded white powder (0.124 g, 0.20 mmol, 28%).

^{1}H NMR (400 MHz, CD_2Cl_2): δ (ppm) = 7.36 (d, J = 8.8 Hz, 4H), 7.31 (d, J = 9.2 Hz, 4H), 7.22 (d, J = 8.8 Hz, 4H), 6.89 (d, J = 8.8 Hz, 4H), 4.17 (m, 4H), 3.74 (m, 4H), 3.58 (m, 4H), 3.53 (m, 4H), 3.5–1.6 (br, 10H).

^{13}C{^{1}H} NMR (100 MHz, CD_2Cl_2): δ (ppm) = 159.3, 142.6, 131.9, 131.6, 128.6, 128.3, 126.1, 115.6, 86.4, 70.9, 70.9, 69.8, 68.2.

^{11}B{^{1}H} NMR (128 MHz, CD_2Cl_2): δ (ppm) = −2.67 (2B), −10.81 (8B).

HRMS (APCI) calcd. for $C_{42}H_{46}B_{10}O_5K_1$ $[M]^-$ 640.3968, found 640.4000.

Synthesis of M2

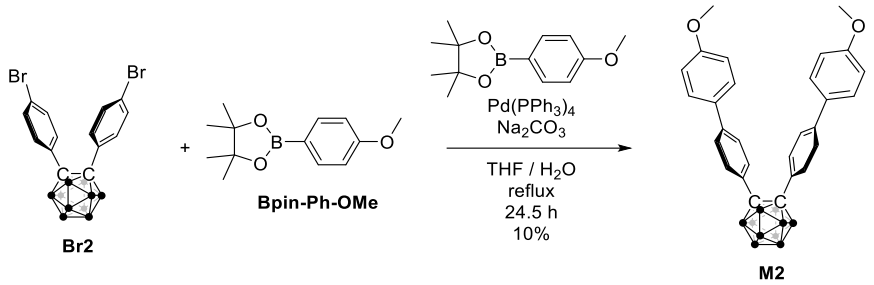

Scheme S4. Synthetic scheme of **M2**.

To a 50 mL 2-necked round-bottom flask, **Br2** (0.091 g, 0.20 mmol), **Bpin-Ph-OMe** (0.141 g, 0.60 mmol), Na_2CO_3 (0.058 g, 0.55 mmol), $Pd(PPh_3)_4$ (0.019 g, 0.016 mmol) was added under N_2 atmosphere. Then, THF (4.0 mL) and H_2O (0.5 mL) was added and refluxed for 24.5 h. After cooling to room temperature, the mixture was extracted with AcOEt. The organic layer was washed with brine and dried over $MgSO_4$. After filtration and evaporation of the solvent to afford brown solid, the crude was supported by silica in $CHCl_3$ and purified by silica gel chromatography (eluent: AcOEt/*n*-hexane = 1/5(v/v)). Recrystallization from MeOH and decantation from hexane afforded light-yellow powder (0.010 g, 0.02 mmol, 10%).

^{1}H NMR (400 MHz, $CDCl_3$): δ (ppm) = 7.49 (d, J = 8.4 Hz, 4H), 7.41 (d, J = 8.4 Hz, 4H), 7.33 (d, J = 8.8 Hz, 4H), 6.91 (d, J = 8.8 Hz, 4H), 3.81 (s, 6H), 3.7–1.6 (br, 10H).
^{13}C{^{1}H} NMR (100 MHz, $CDCl_3$): δ (ppm) = 159.7, 142.3, 131.6, 131.0, 129.0, 128.1, 126.2, 114.3 85.4, 55.3.
^{11}B{^{1}H} NMR (128 MHz, $CDCl_3$): δ (ppm) = −2.36 (4B), −10.54 (6B).
HRMS (APCI) calcd. for $C_{28}H_{32}B_{10}O_2$ $[M]^-$ 510.3338, found 510.3362.

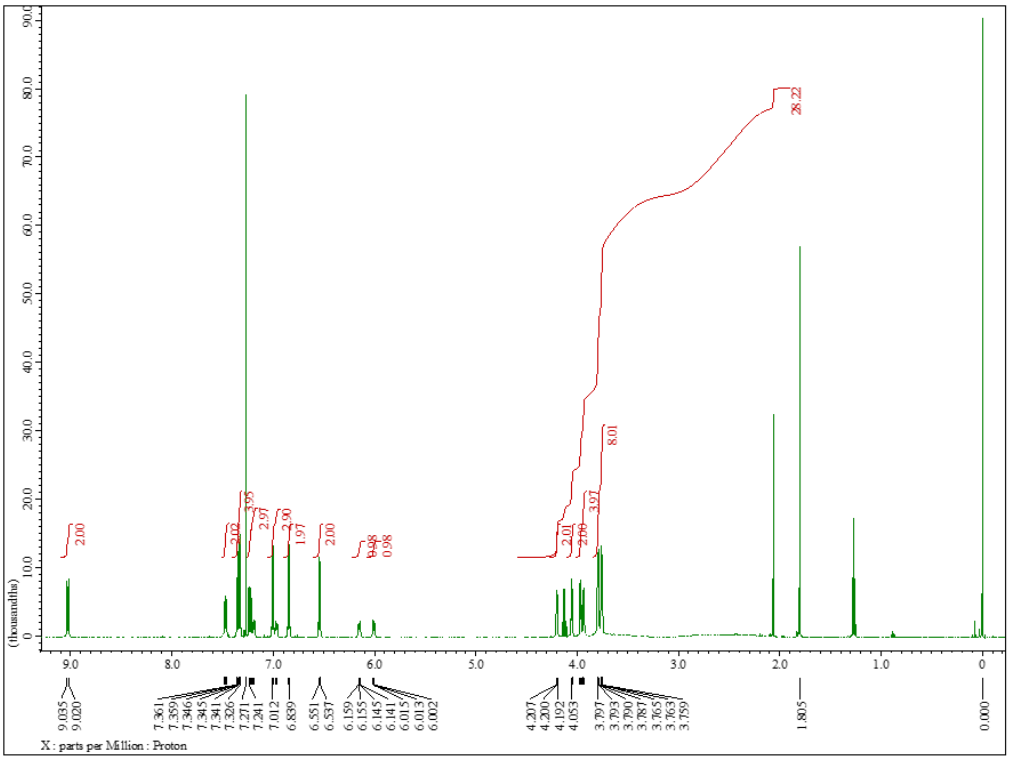

Chart S1. ^{1}H NMR spectrum of **C1** in $CDCl_3$ at 0 ºC.

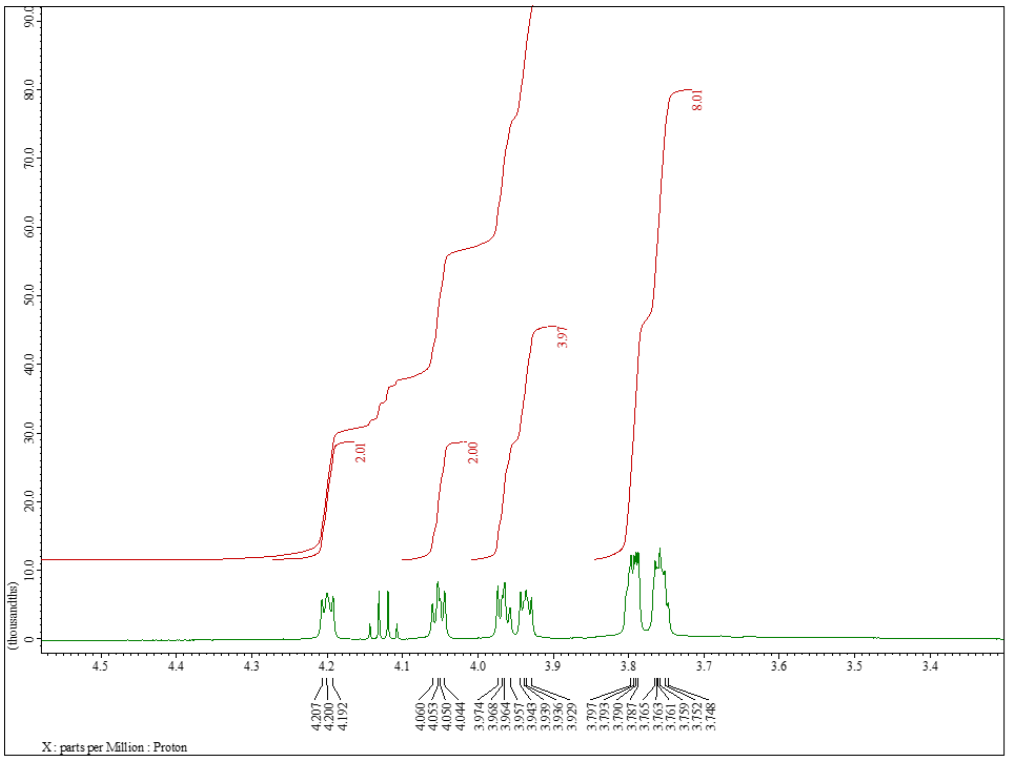

Chart S2. ^{1}H NMR spectrum of **C1** (TEG protons) in $CDCl_3$ at 0 ºC.

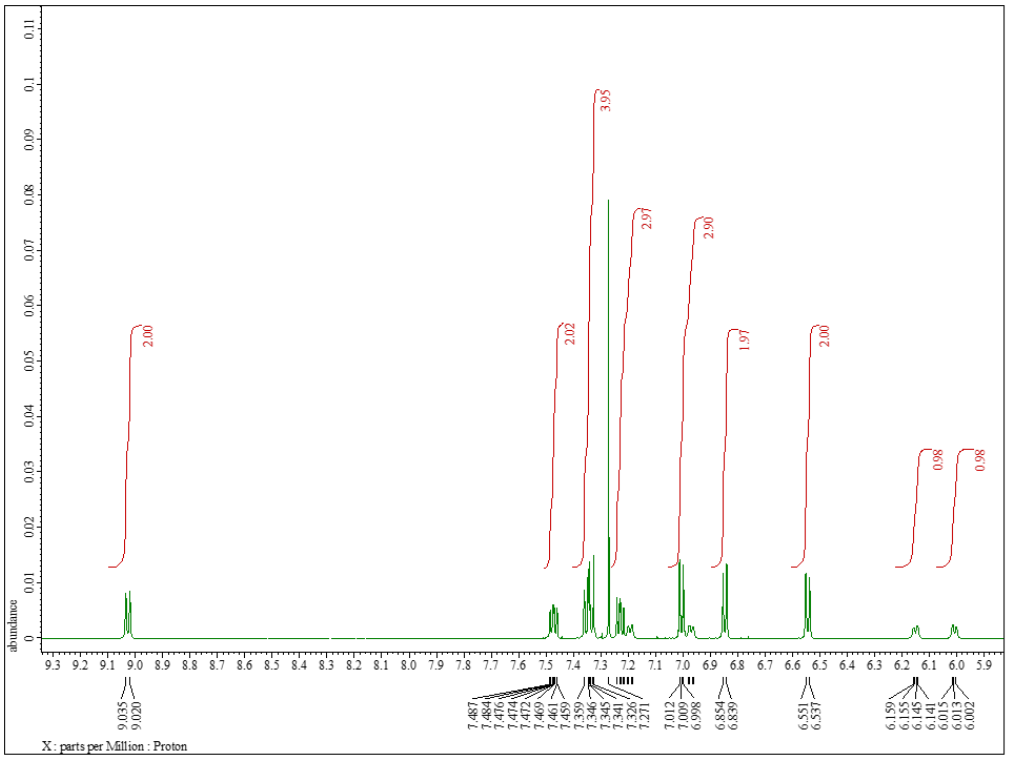

Chart S3. ^{1}H NMR spectrum of **C1** (aromatic protons) in $CDCl_3$ at 0 ºC.

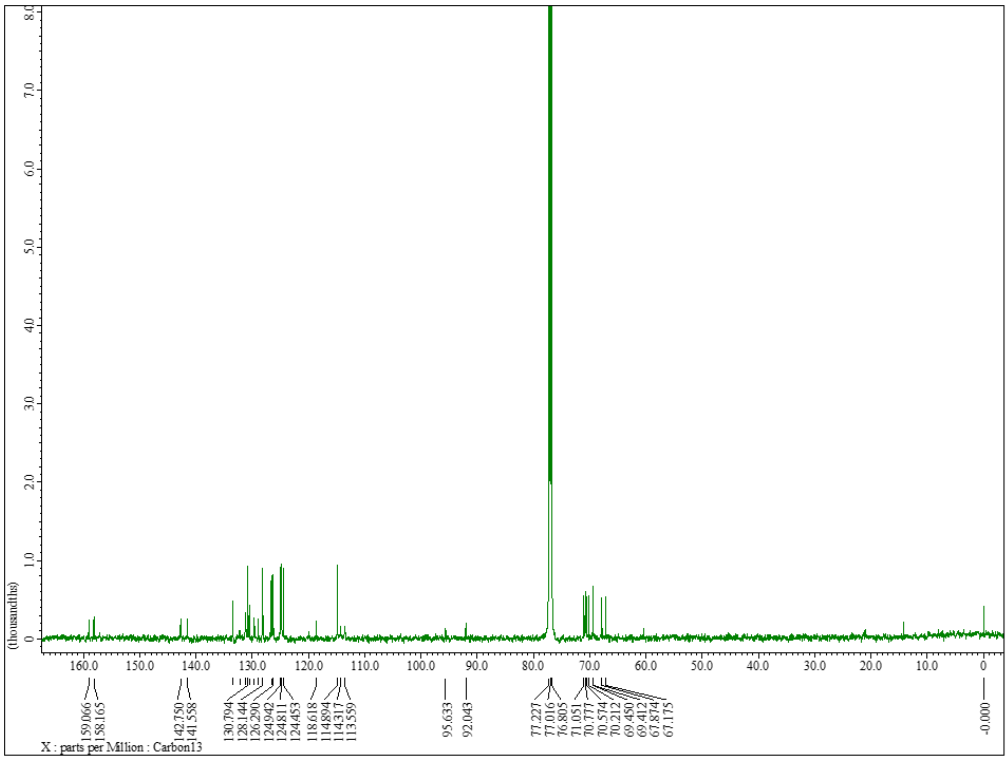

Chart S4. $^{13}C\{^{1}H\}$ NMR spectrum of **C1** in $CDCl_3$ at 0 ºC.

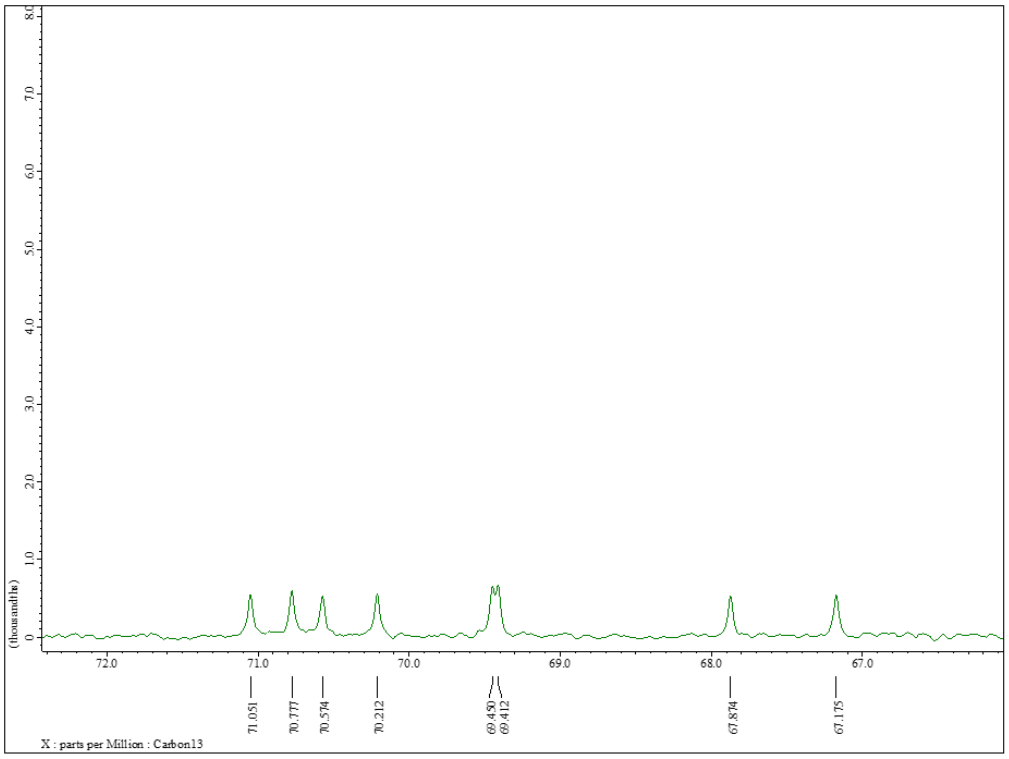

Chart S5. $^{13}C\{^{1}H\}$ NMR spectrum of **C1** (TEG carbons) in $CDCl_3$ at 0 ºC.

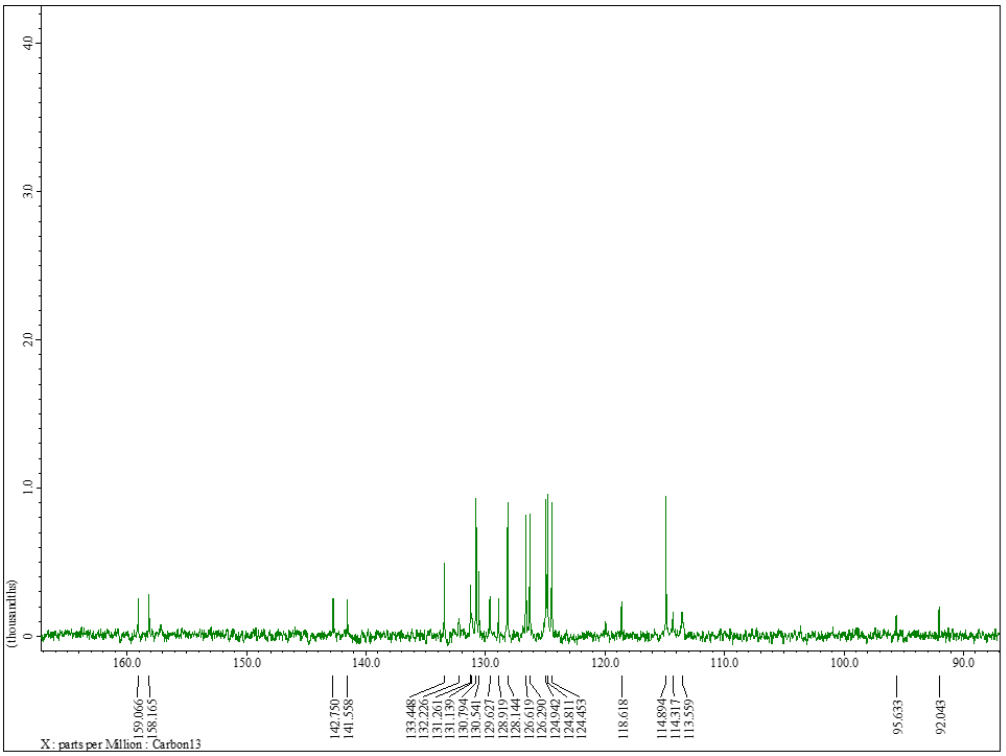

Chart S6. $^{13}C\{^{1}H\}$ NMR spectrum of **C1** (aromatic and C_{cage} carbons) in $CDCl_3$ at 0 ºC.

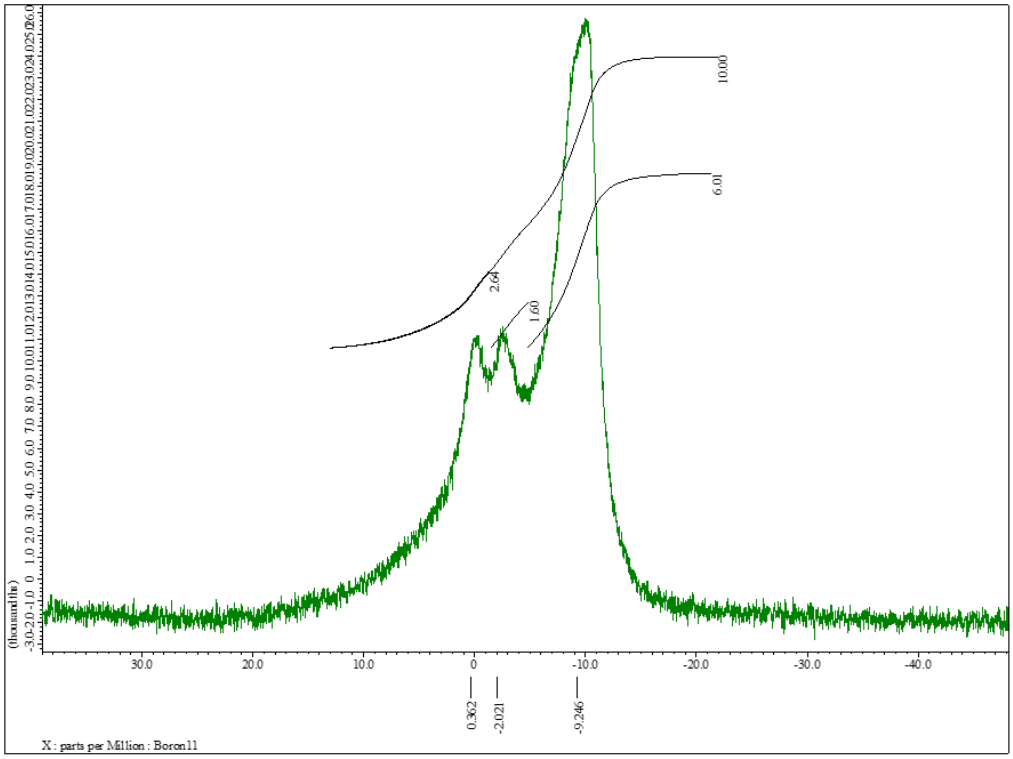

Chart S7. $^{11}B\{^{1}H\}$ NMR spectrum of **C1** in $CDCl_3$ at r.t.

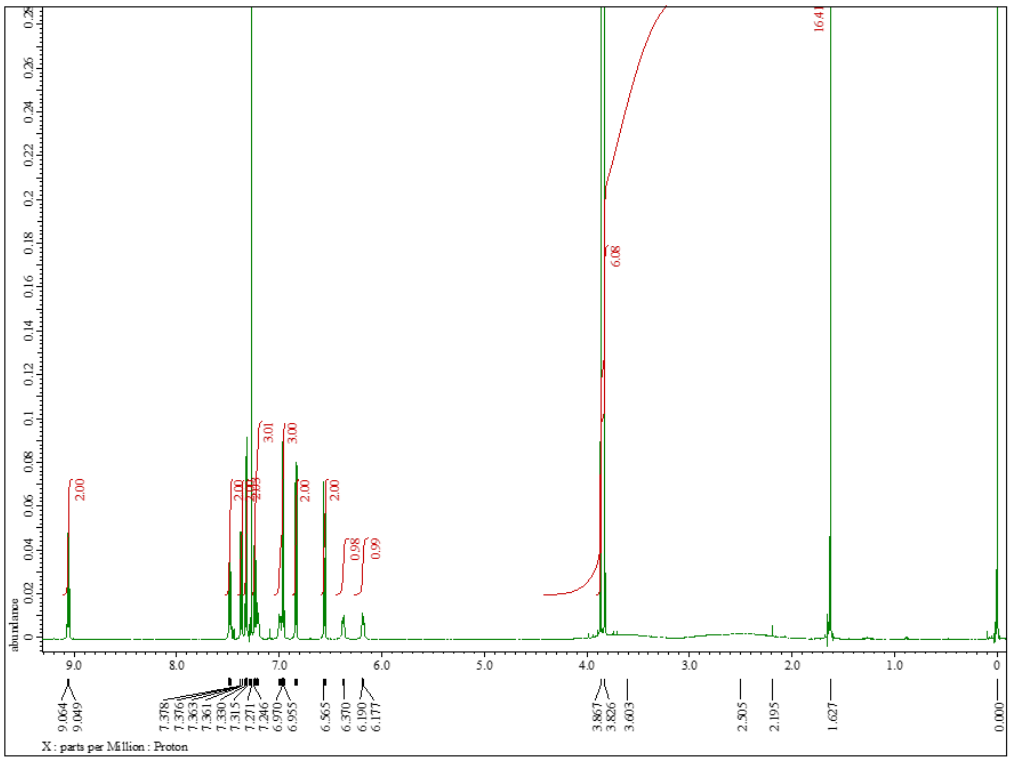

Chart S8. ^{1}H NMR spectrum of **M1** in $CDCl_3$ at 0 ºC.

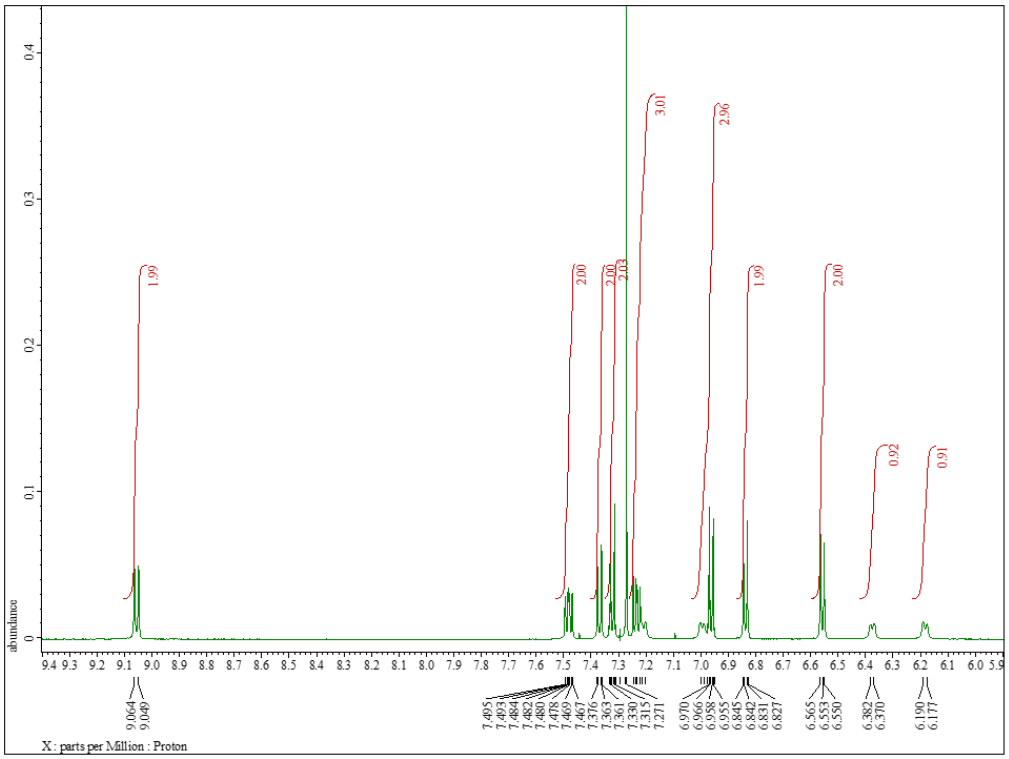

Chart 9. ^{1}H NMR spectrum of **M1** (aromatic protons) in $CDCl_3$ at 0 ºC.

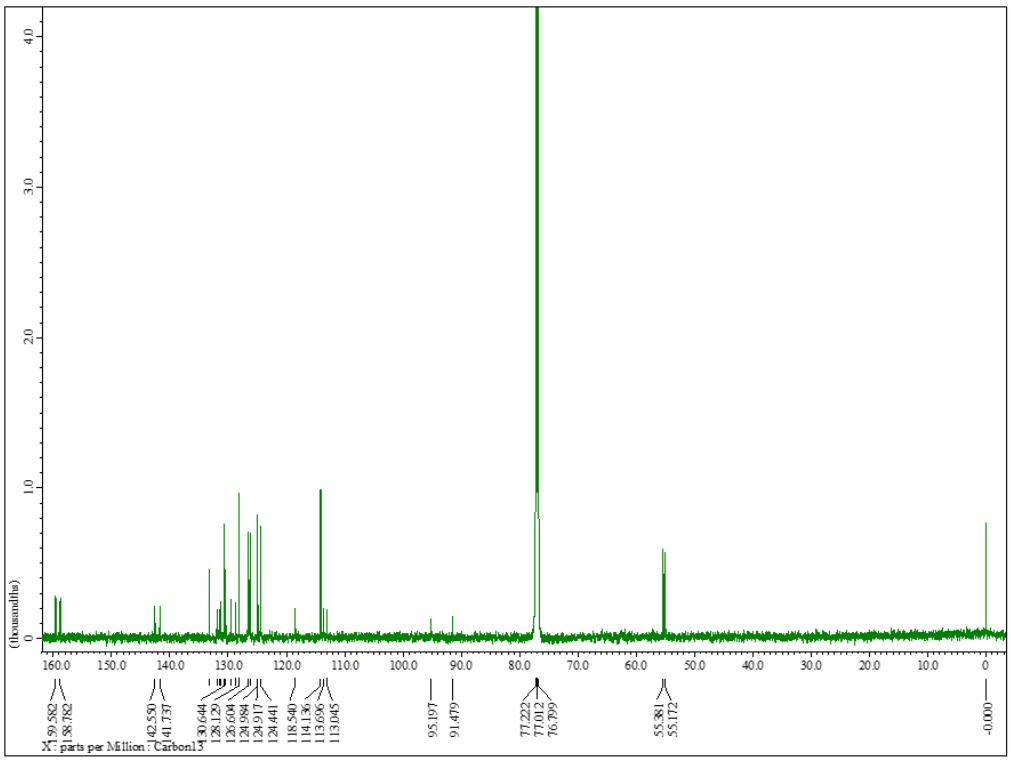

Chart S10. ^{13}C{^{1}H} NMR spectrum of **M1** in $CDCl_3$ at 0 ºC.

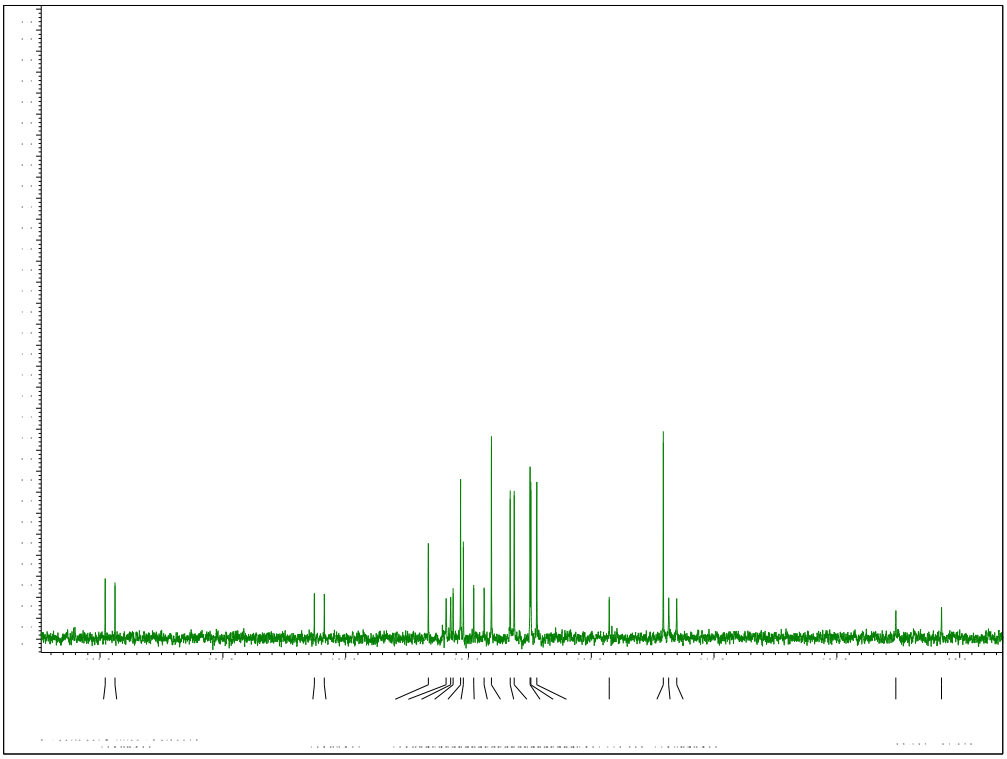

Chart S11. $^{13}C\{^{1}H\}$ NMR spectrum of **M1** (aromatic and C_{cage} carbons) in $CDCl_3$ at 0 ºC.

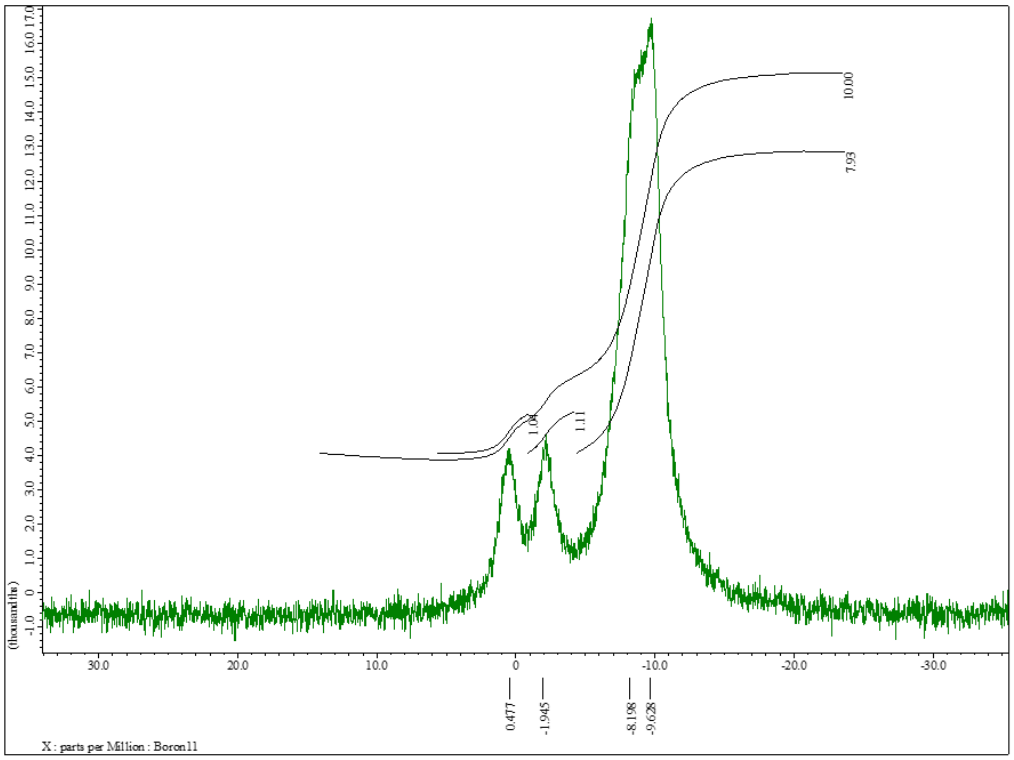

Chart S12. $^{11}B\{^{1}H\}$ NMR spectrum of **M1** in $CDCl_3$ at r.t.

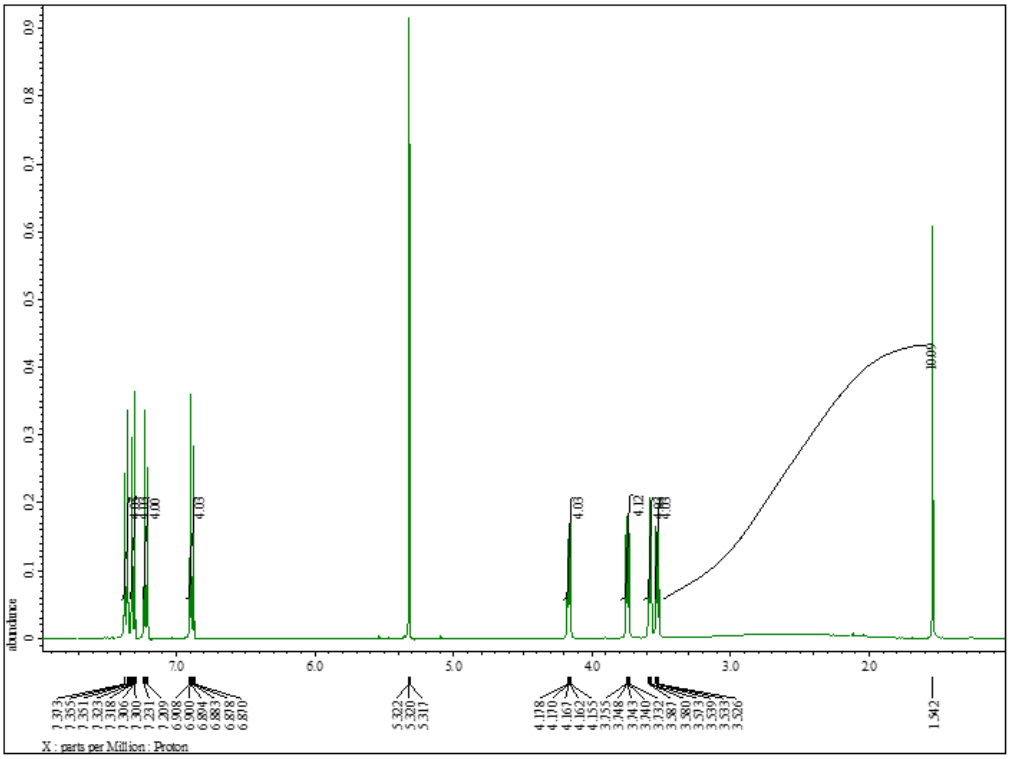

Chart S13. ^{1}H NMR spectrum of **C2** in CD_2Cl_2 at r.t.

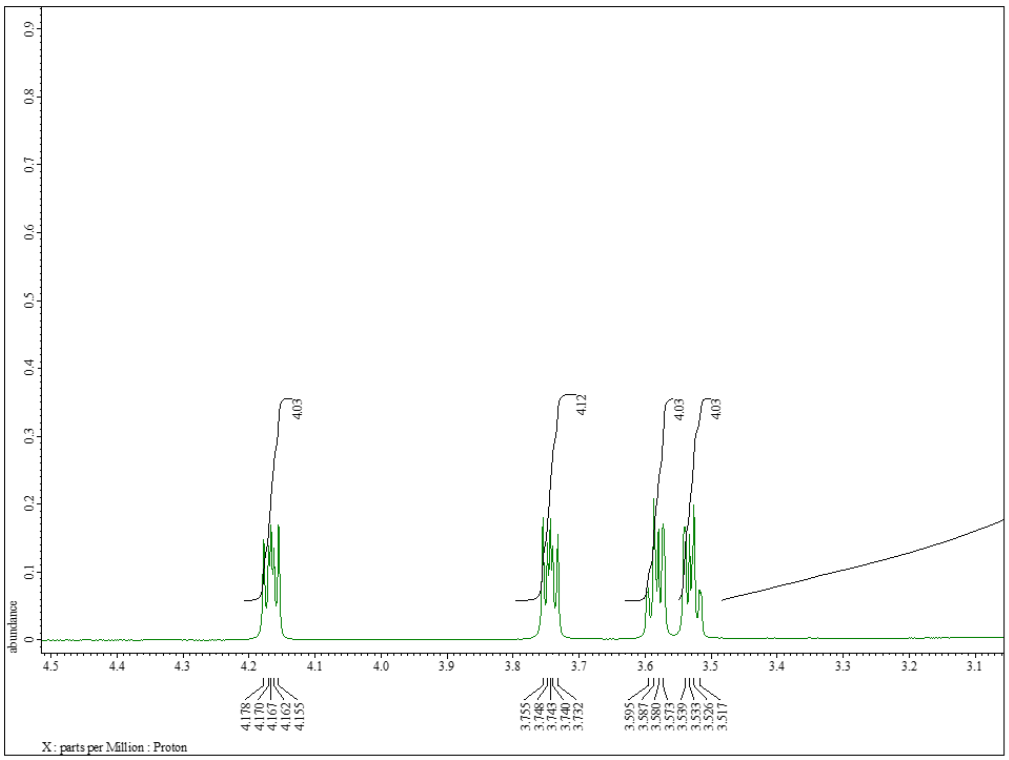

Chart S14. ^{1}H NMR spectrum of **C2** (TEG protons) in CD_2Cl_2 at r.t.

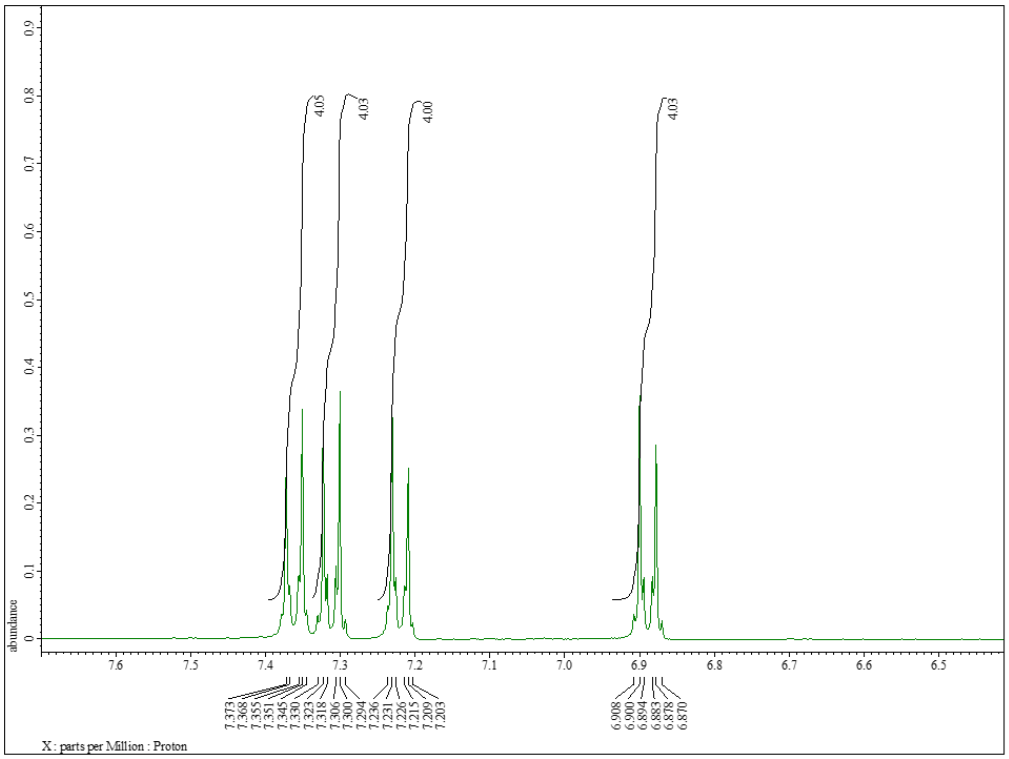

Chart 15. ^{1}H NMR spectrum of **C2** (aromatic protons) in CD_2Cl_2 at r.t.

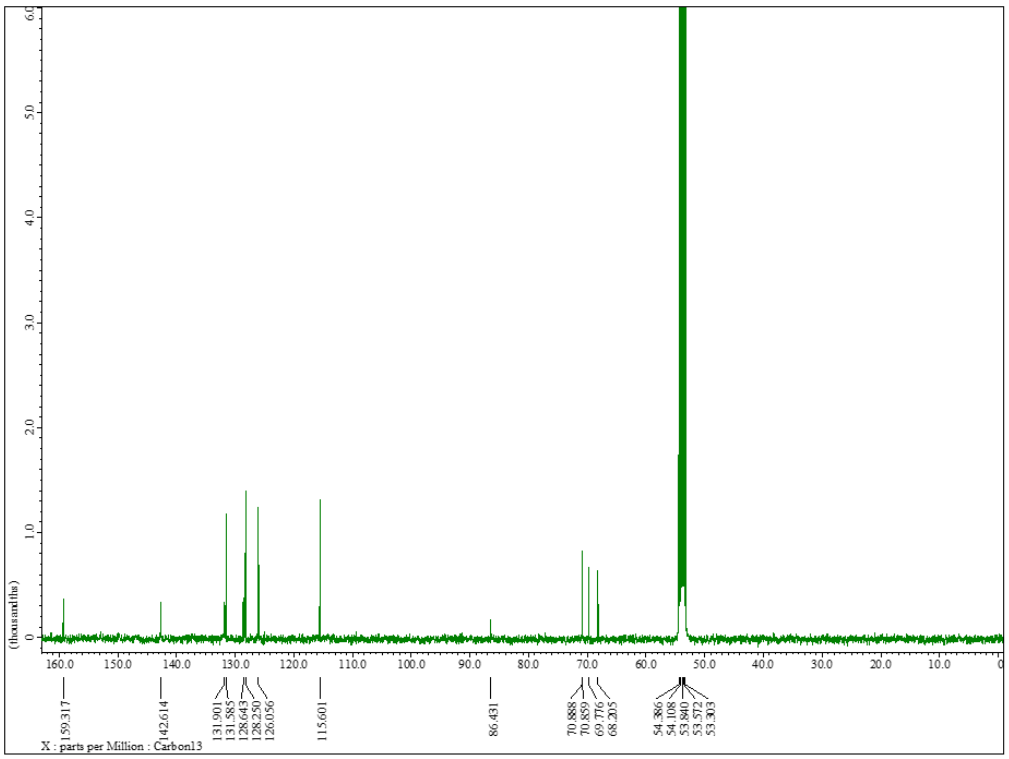

Chart S16. ^{13}C{^{1}H} NMR spectrum of **C2** in CD_2Cl_2 at r.t.

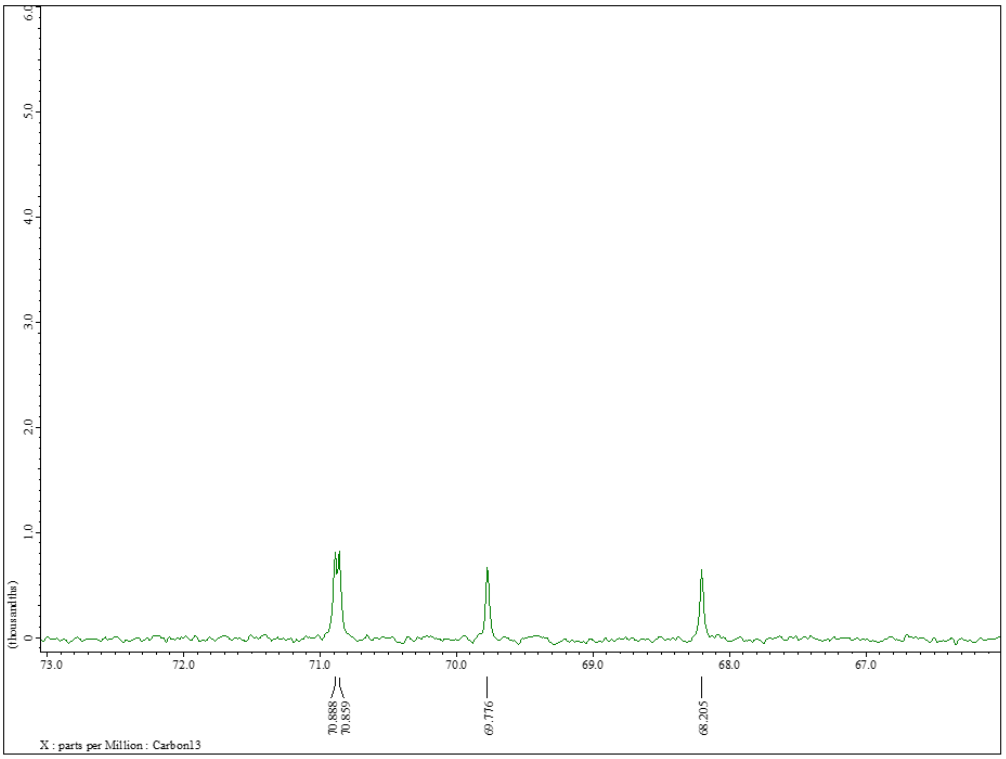

Chart S17. $^{13}C\{^{1}H\}$ NMR spectrum of **C2** (TEG carbons) in CD_2Cl_2 at r.t.

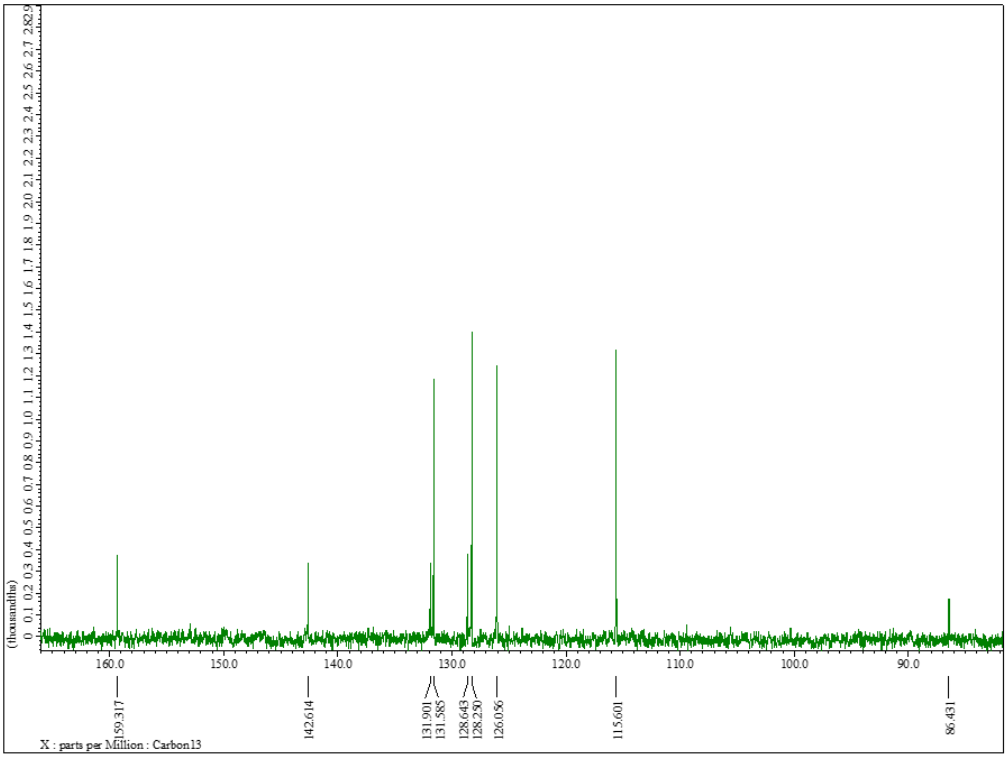

Chart S18. $^{13}C\{^{1}H\}$ NMR spectrum of **C2** (aromatic and C_{cage} carbons) in CD_2Cl_2 at r.t.

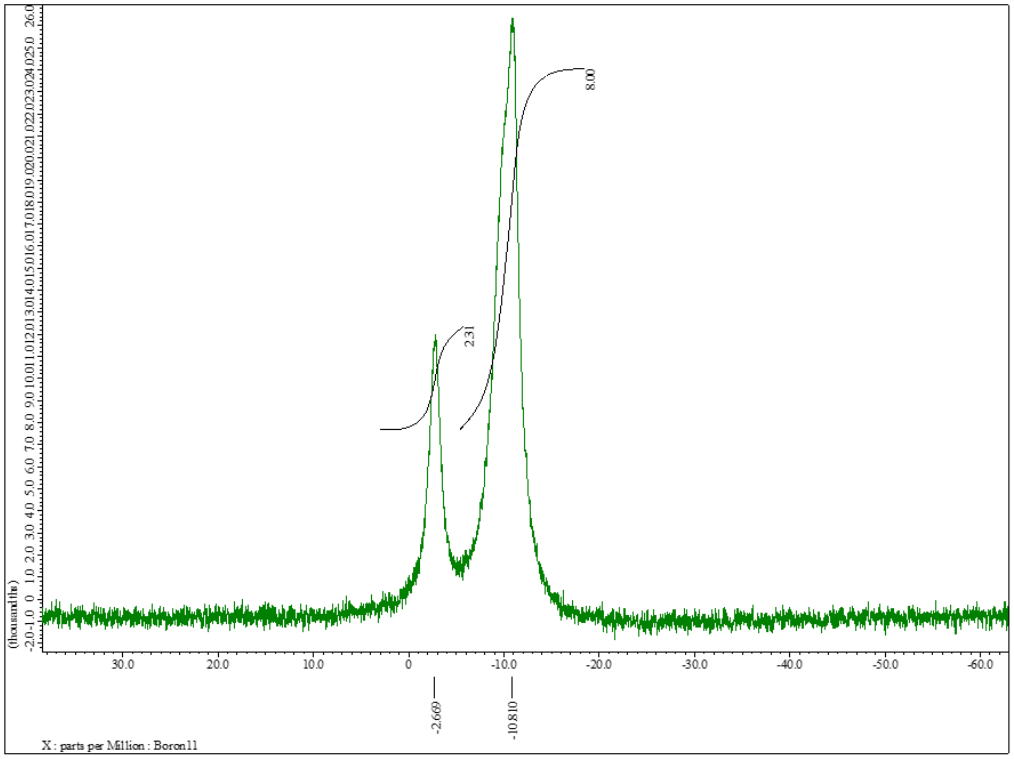

Chart S19. $^{11}B\{^{1}H\}$ NMR spectrum of **C2** in CD_2Cl_2 at r.t.

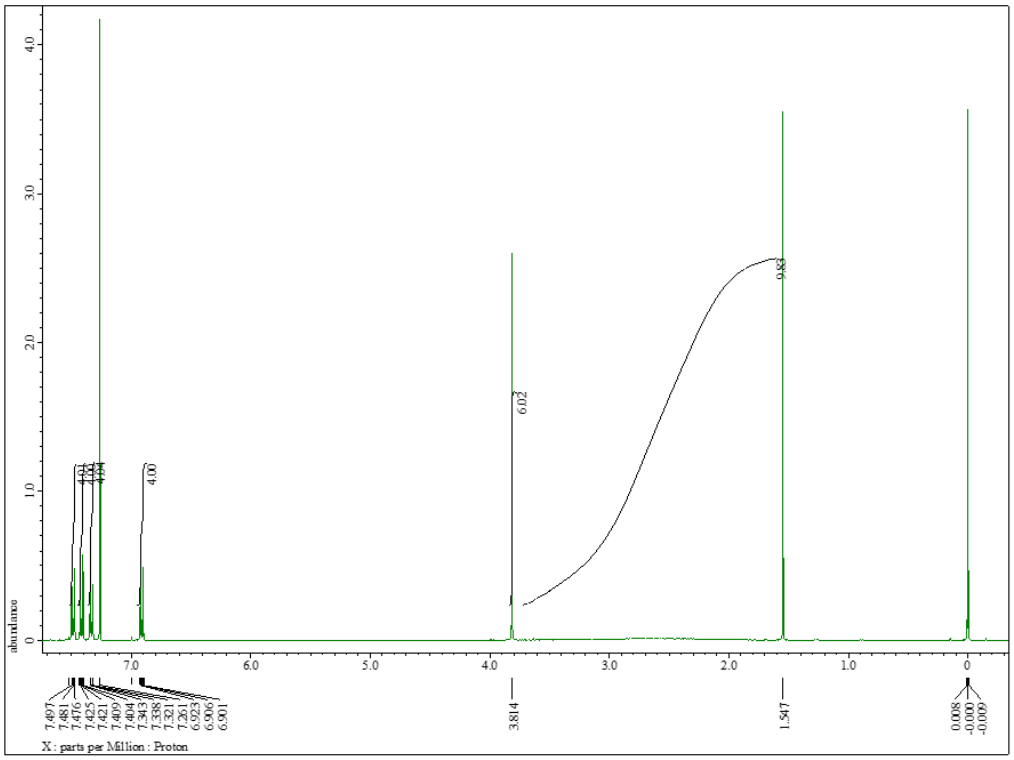

Chart S20. ^{1}H NMR spectrum of **M2** in $CDCl_3$ at r.t.

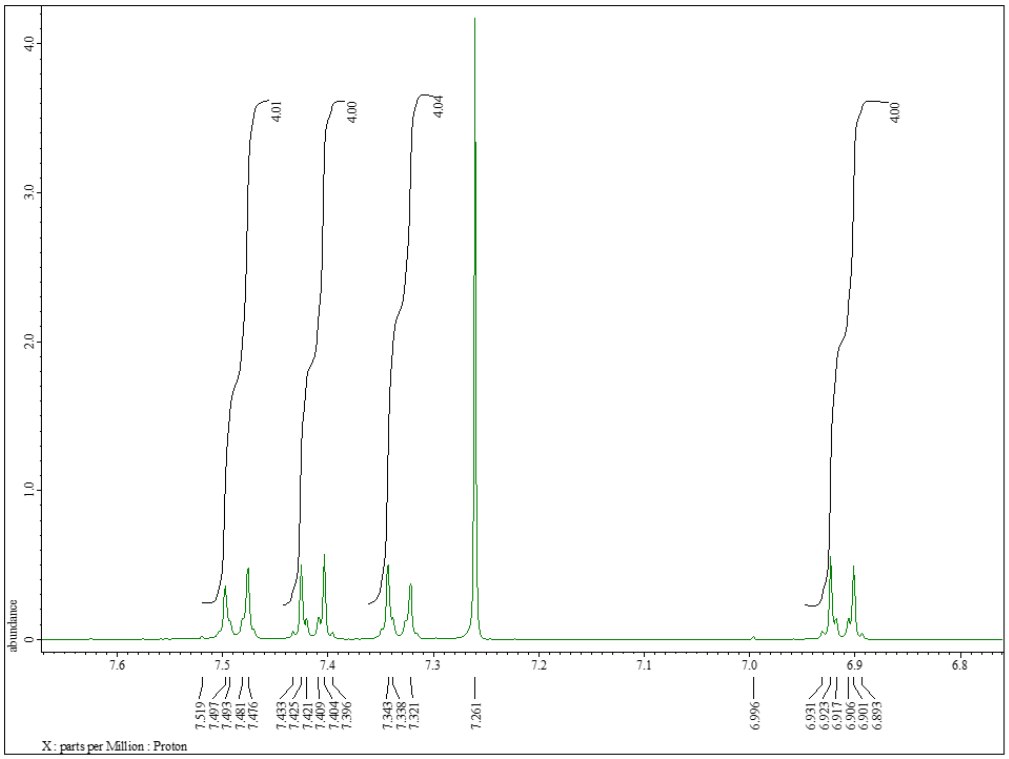

Chart S21. ^{1}H NMR spectrum of **M2** (aromatic protons) in $CDCl_3$ at r.t.

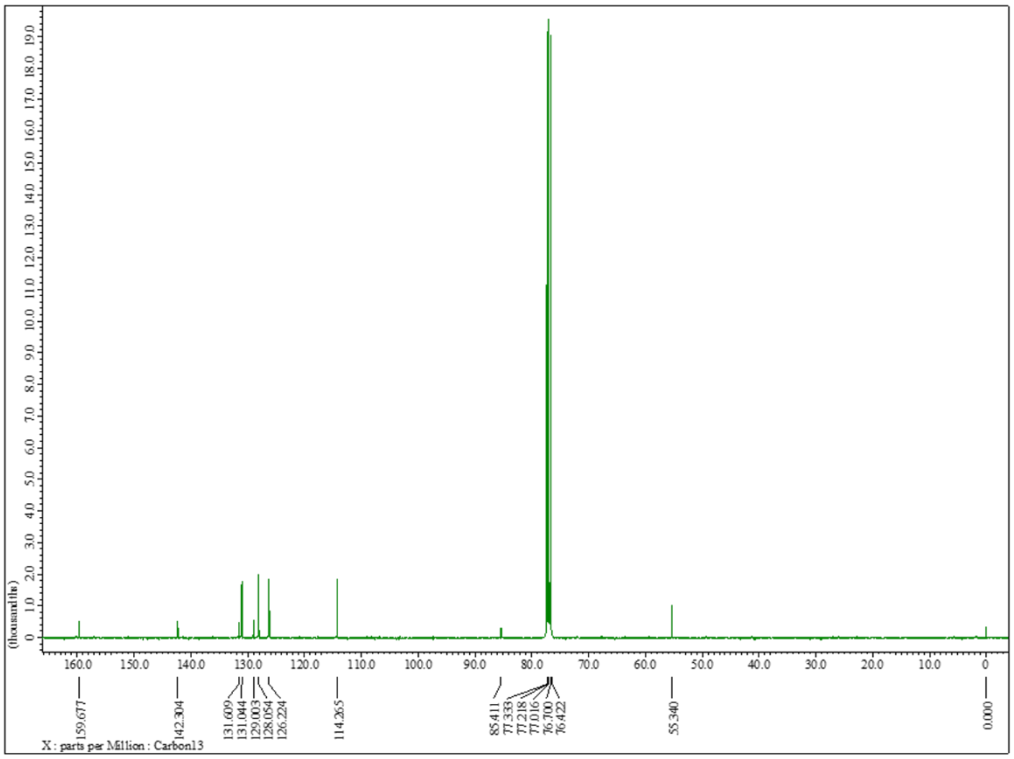

Chart S22. $^{3}C\{^{1}H\}$ NMR spectrum of **M2** in $CDCl_3$ at r.t.

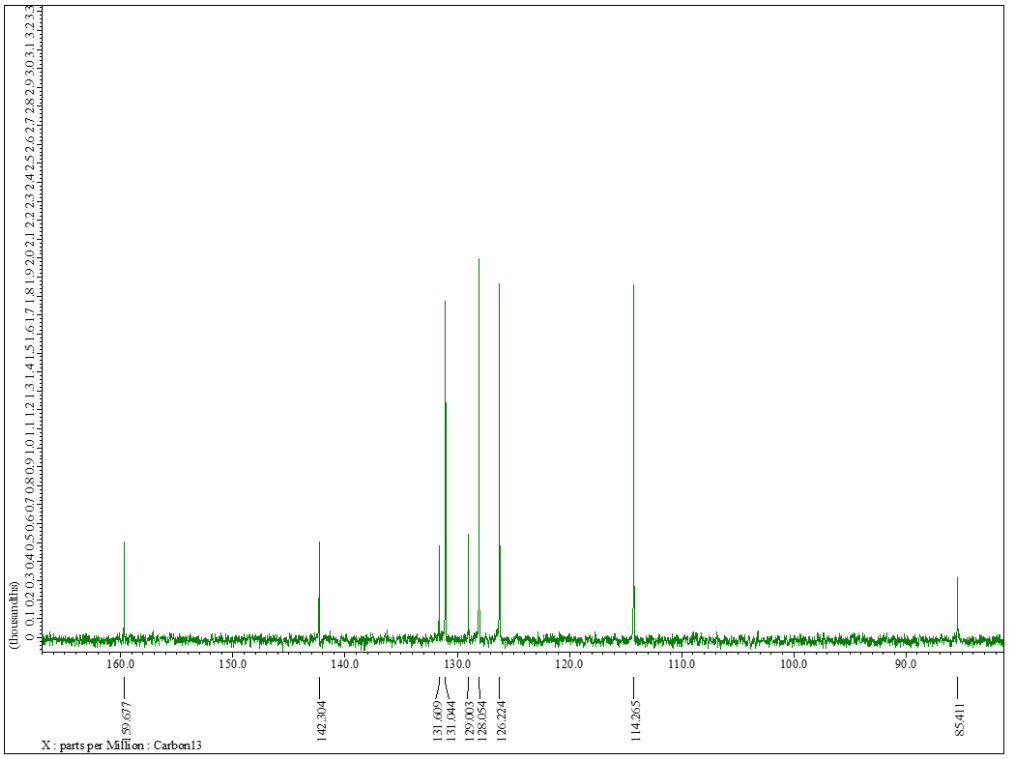

Chart S23. $^{13}C\{^{1}H\}$ NMR spectrum of **M2** (aromatic and C_{cage} carbons) in $CDCl_3$ at r.t.

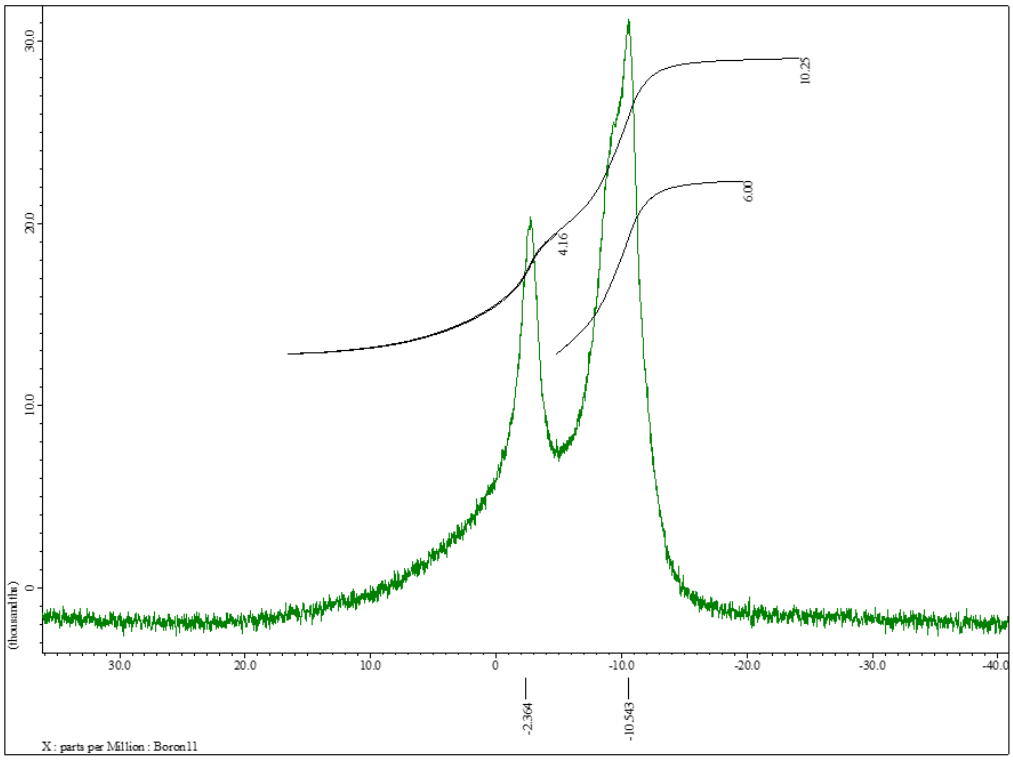

Chart S24. $^{11}B\{^{1}H\}$ NMR spectrum of **M2** in $CDCl_3$ at r.t.

Single-Crystal X-ray Diffraction Analysis

Table S1. Crystallographic data of **M1** (CCDC No. 2451167)

Empirical formula	$C_{36}H_{36}B_{10}O_2$
Formula weight	608.75
Temperature (K)	143
Wavelength (Å)	0.71075
Crystal system, space group	Monoclinic, $P2_1/n$
Unit cell dimensions	a = 13.613(3)
	b = 27.741(6)
	c = 18.688(4)
	α = 90
	β = 111.778(3)
	γ = 90
V (Å^3)	6554(3)
Z, calculated density (Mg m^{-3})	8, 1.234
Absorption coefficient	0.069
F(000)	2544
Crystal size (mm)	0.27×0.11×0.03
θ range for data collection	3.082–27.587
Limiting indices	$-17\leq h\leq 15$, $-36\leq k\leq 36$, $-19\leq l\leq 24$
Reflections collected (unique) [a]	52835/14927 [R_{int} = 0.0679]
S (Goodness-of-fit on F^2) [b]	1.147
Final R indices [$I > 2\sigma(I)$] [c,d]	R_1 = 0.0750, wR_2 = 0.1333
R indices (all data) [c,d]	R_1 = 0.1086, wR_2 = 0.1480

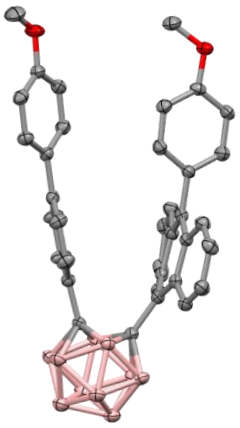

[a] $R_{int} = \Sigma||F_0|^2-<|F_o|^2>|/\Sigma|F_o|^2$ [b] $S = [\{\Sigma w(|F_0|^2-|F_c|^2)^2\}/(N_o - N_p)]^{1/2}$ [c] $R_1 = [\Sigma(|F_0|^2-|F_c|^2)^2/\Sigma(|F_0|^2)^2]^{1/2}$

[d] $wR_2 = [\Sigma w(|F_0|^2-|F_c|^2)^2/\Sigma w(|F_0|^2)^2]^{1/2}$. $w = 1/[\sigma^2(|F_0|^2)+[(ap)^2+bp]]$, where $p = [|F_0|^2,+2|F_c|^2]/3$

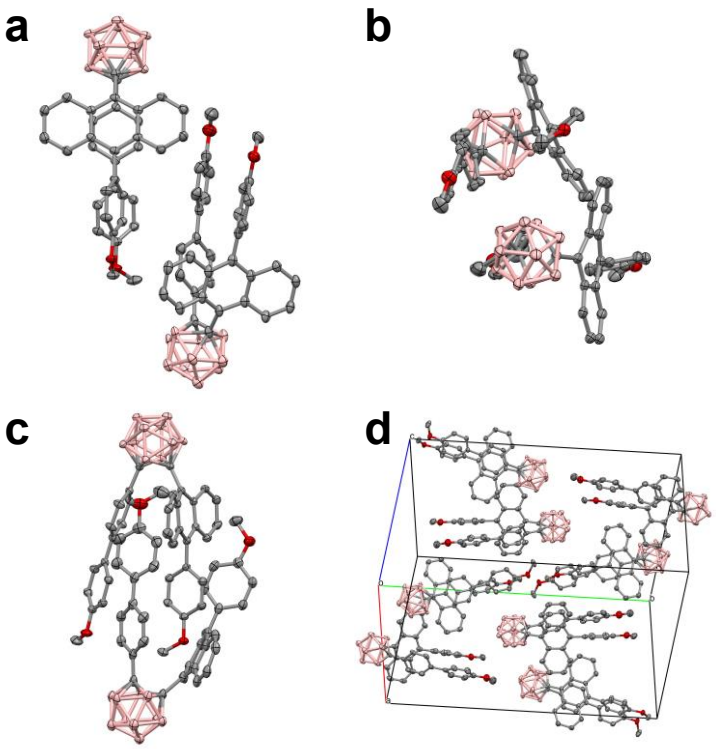

Figure S1. ORTEP drawings of **M1**. (a) Front, (b) top, and (c) side view of the asymmetric unit. (d) packing of the unit cell. Thermal ellipsoids are drawn at 50% probability level. Hydrogen atoms are omitted for clarity. Colors: B, pink; C, grey; O, red.

Powder X-ray Diffraction Analyses

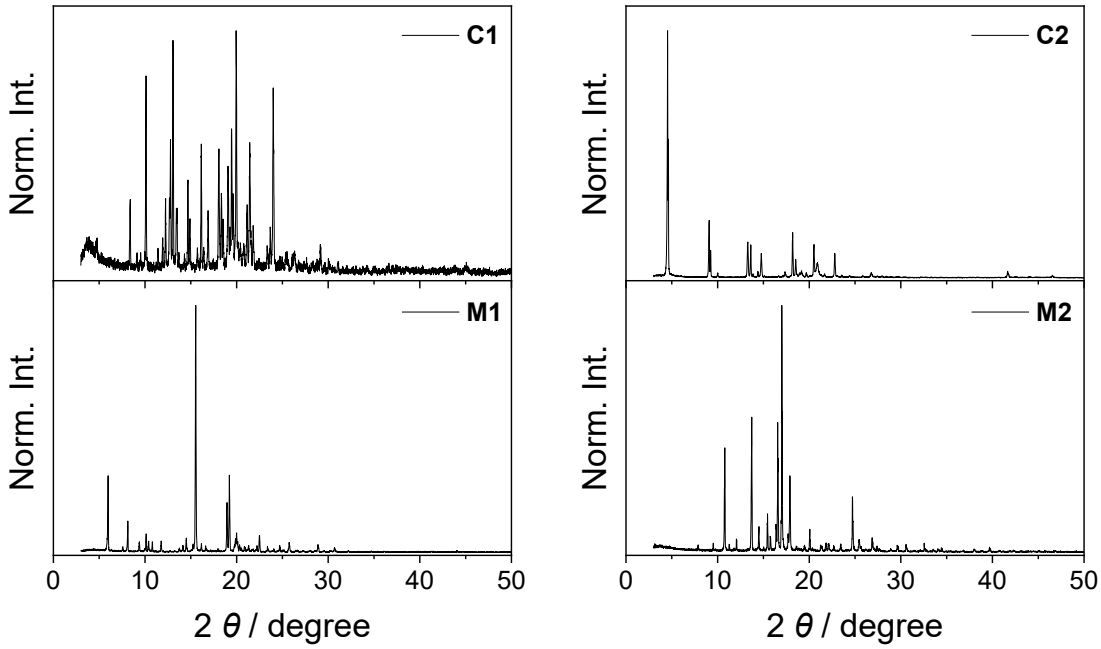

Figure S2. PXRD patterns of **C1**, **C2**, **M1**, and **M2**.

NMR Titration and Job Plot

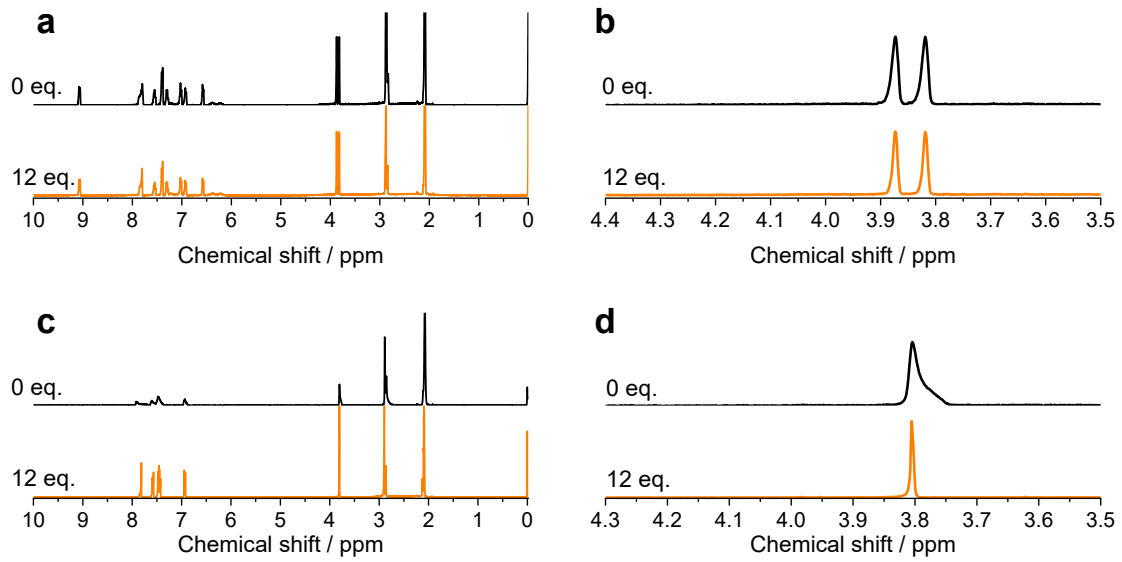

Figure S3. ^{1}H NMR spectra of (a,b) **M1** and (c,d) **M2** with hexafluorophosphate salt of K^{+} (0 and 12 eq.) in 2.0×10^{-3} M acetone-d_6/$CDCl_3$ (3/2, v/v) solution. (a,c) all region and (b,d) enlarged region.

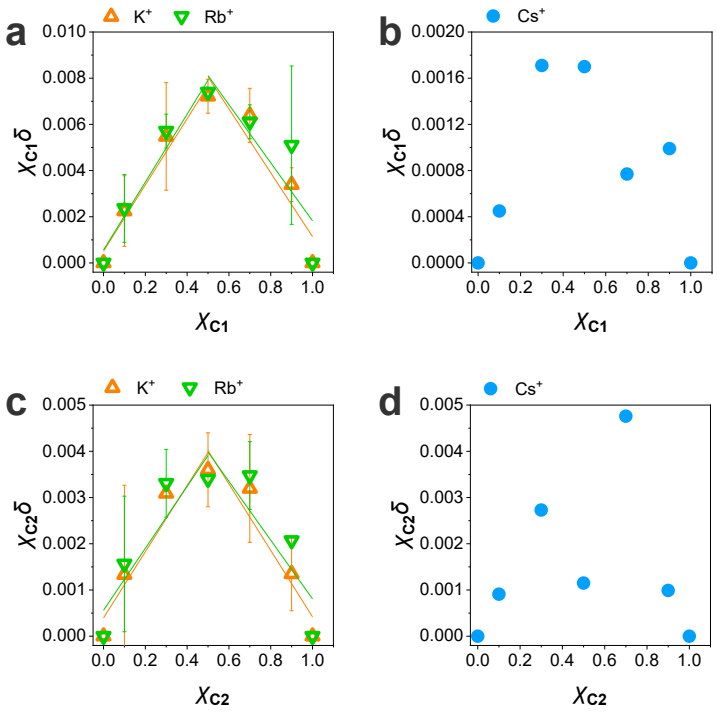

Figure S4. Job plots obtained from ^{1}H NMR measurements of (a, b) **C1** and (c, d) **C2** with hexafluorophosphate salt of (a, c) K^{+} and Rb^{+}, and (b, d) Cs^{+}. Error bars represent standard deviation of uncertainty.

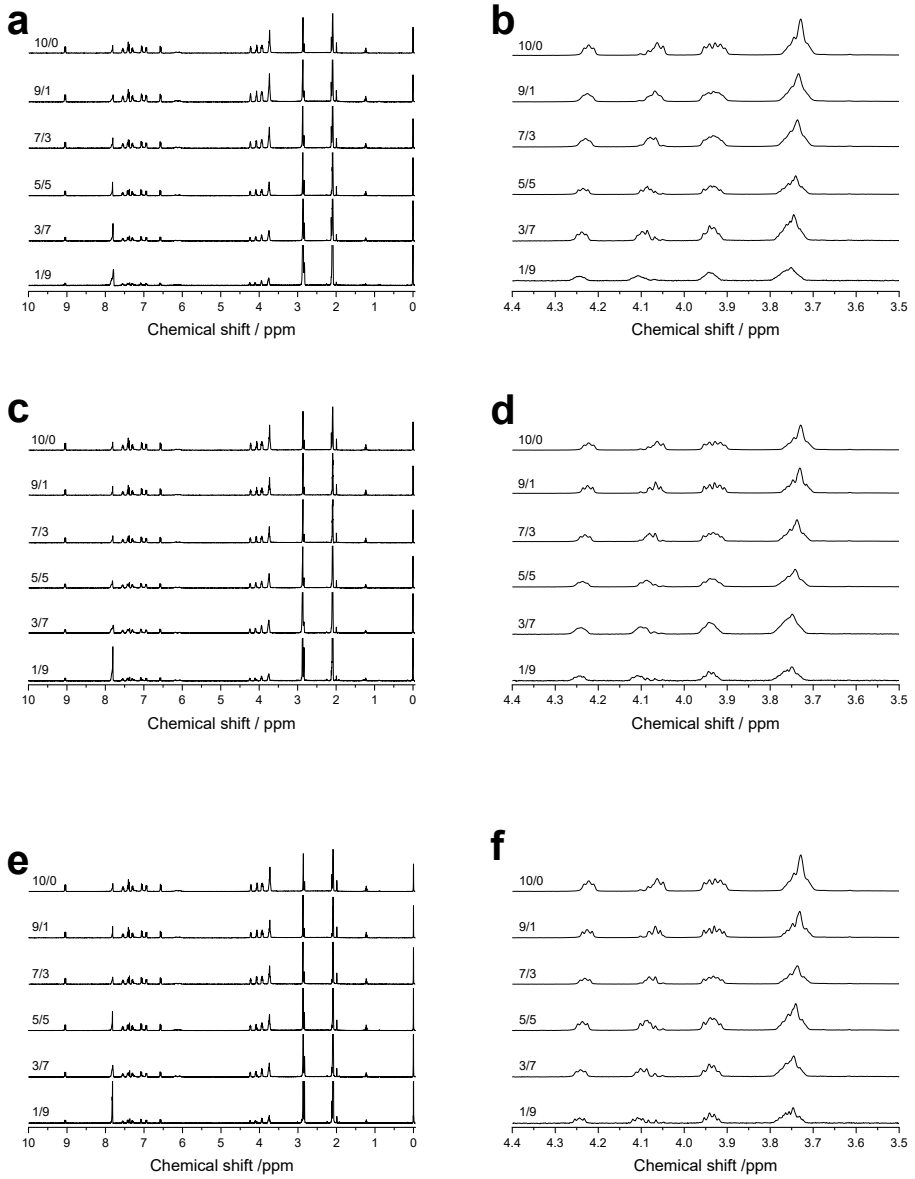

Figure S5. ^{1}H NMR spectra of **C1** with hexafluorophosphate salt of K^+ ([**C1**]/K^+ = 10/0, 9/1, 7/3, 5/5, 3/7, and 1/9) in acetone-d_6/$CDCl_3$ (3/2, v/v). [**C1**] + [KPF_6] = 4 mM. (a,c,e) all region and (b,d,f) enlarged region. The titration was performed three times (1st (a,b), 2nd (c,d), 3rd (e,f)) to guarantee the accuracy of Job plots.

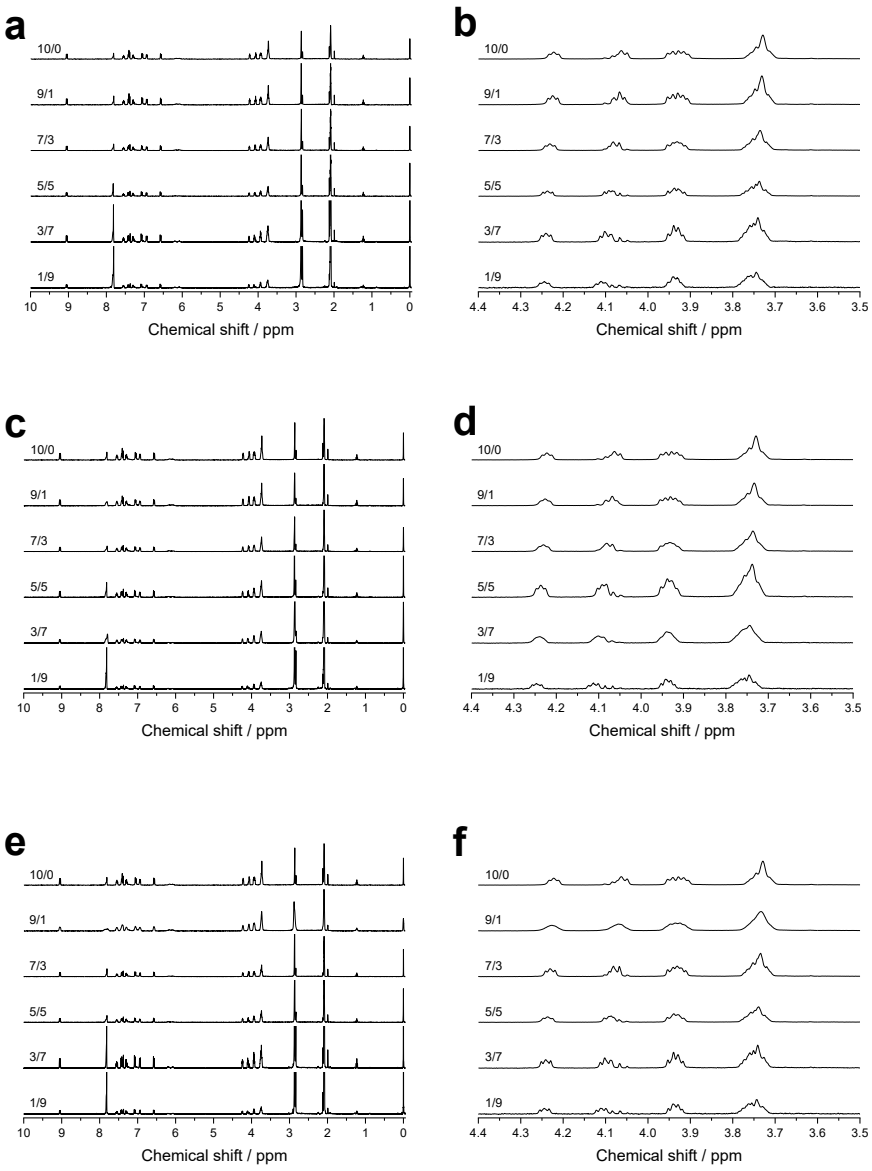

Figure S6. ^{1}H NMR spectra of **C1** with hexafluorophosphate salt of Rb^{+} ([**C1**]/[Rb^{+}] = 10/0, 9/1, 7/3, 5/5, 3/7, and 1/9) in acetone-d_6/$CDCl_3$ (3/2, v/v). [**C1**] + [$RbPF_6$] = 4 mM. (a,c,e) all region and (b,d,f) enlarged region. The titration was performed three times (1st (a,b), 2nd (c,d), 3rd (e,f)) to guarantee the accuracy of Job plots.

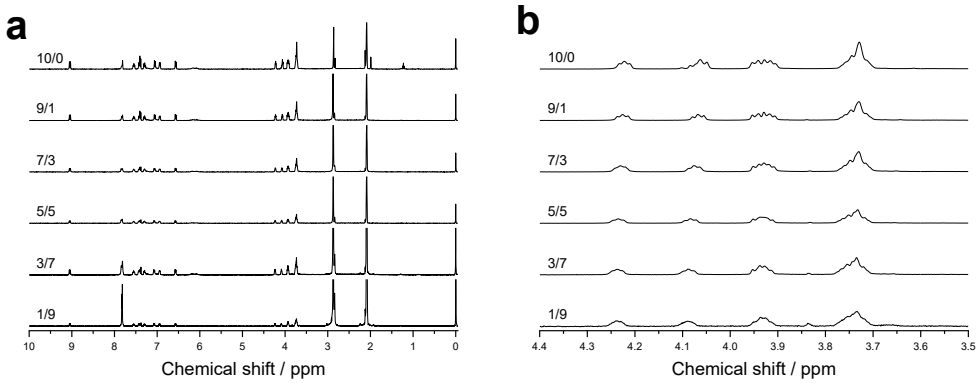

Figure S7. ^{1}H NMR spectra of **C1** with hexafluorophosphate salt of Cs^{+} ([**C1**]/[Cs^{+}] = 10/0, 9/1, 7/3, 5/5, 3/7, and 1/9) in acetone-d_6/$CDCl_3$ (3/2, v/v). [**C1**] + [$CsPF_6$] = 4 mM. (a) all region and (d) enlarged region.

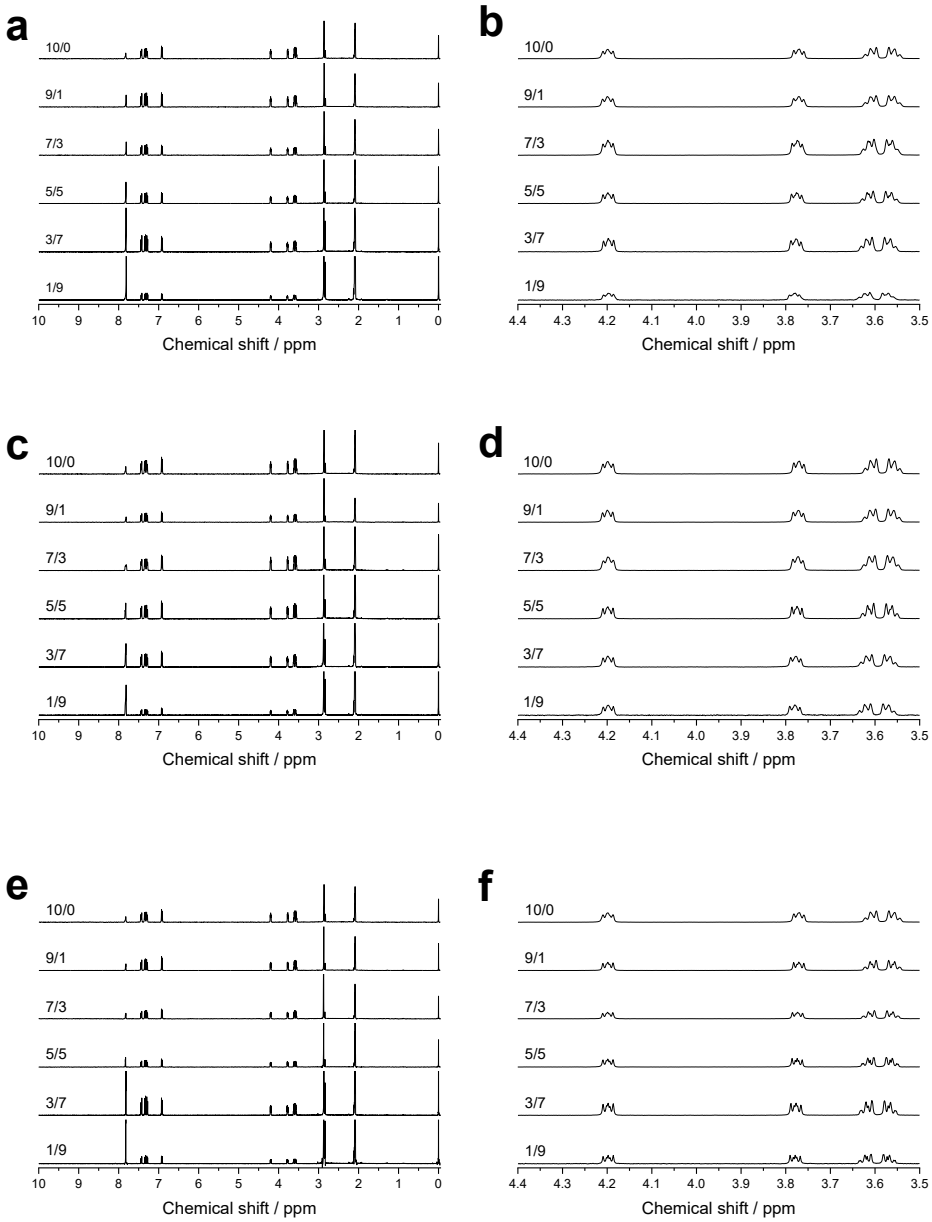

Figure S8. ^{1}H NMR spectra of **C2** with hexafluorophosphate salt of K^+ ([**C2**]/[K^+] = 10/0, 9/1, 7/3, 5/5, 3/7, and 1/9) in acetone-d_6/$CDCl_3$ (3/2, v/v). [**C2**] + [KPF_6] = 4 mM. (a,c,e) all region and (b,d,f) enlarged region. The titration was performed three times (1st (a,b), 2nd (c,d), 3rd (e,f)) to guarantee the accuracy of Job plots.

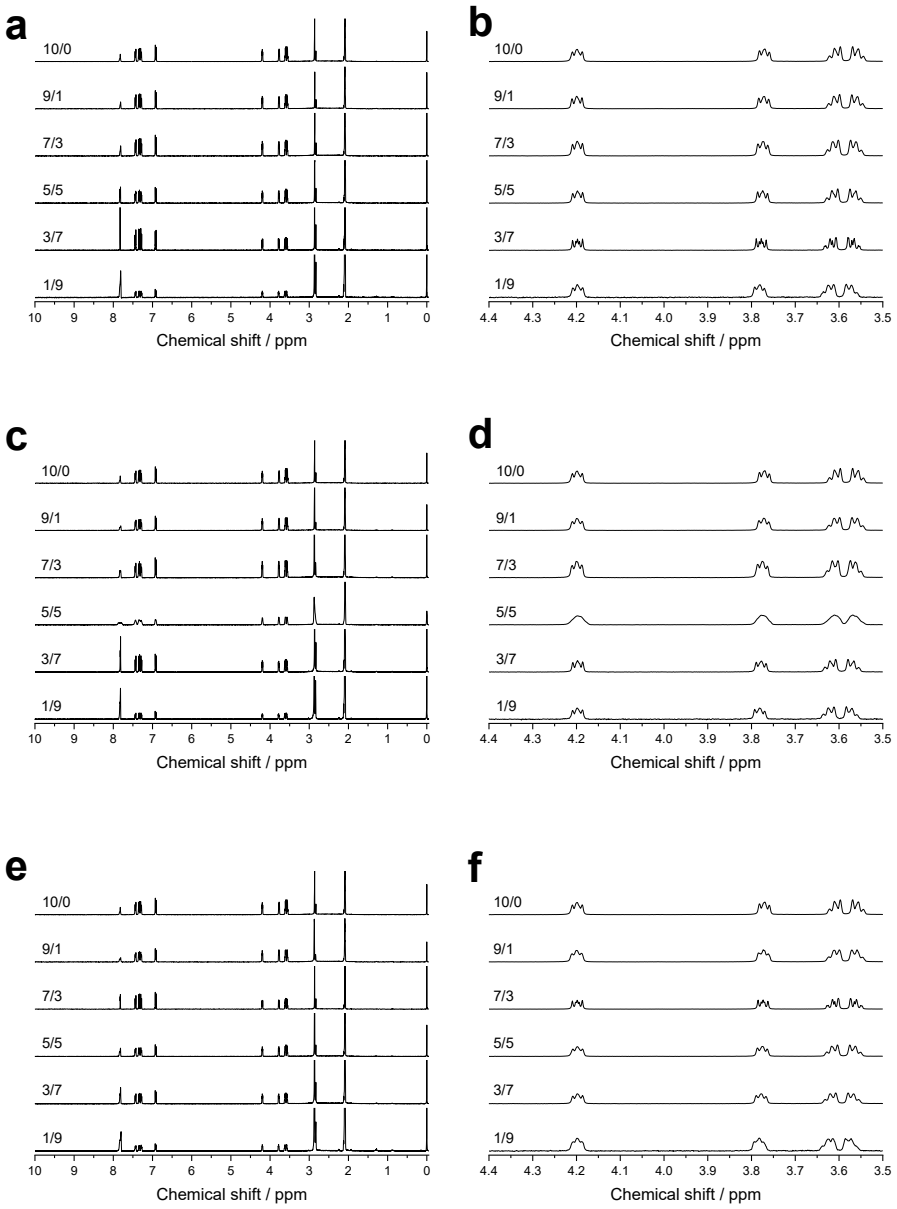

Figure S9. ^{1}H NMR spectra of **C2** with hexafluorophosphate salt of Rb^{+} ([**C2**]/[Rb^{+}] = 10/0, 9/1, 7/3, 5/5, 3/7, and 1/9) in acetone-d_6/$CDCl_3$ (3/2, v/v). [**C2**] + [$RbPF_6$] = 4 mM. (a,c,e) all region and (b,d,f) enlarged region. The titration was performed three times (1st (a,b), 2nd (c,d), 3rd (e,f)) to guarantee the accuracy of Job plots.

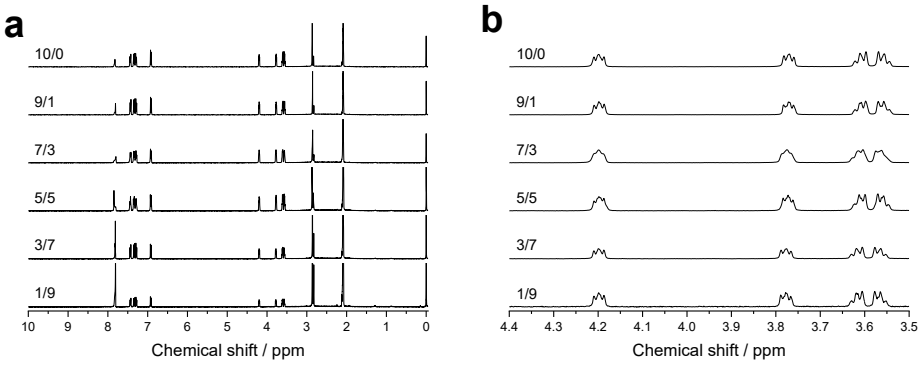

Figure S10. ^{1}H NMR spectra of **C2** with hexafluorophosphate salt of Cs^+ ([**C2**]/[Cs^+] = 10/0, 9/1, 7/3, 5/5, 3/7, and 1/9) in acetone-d_6/$CDCl_3$ (3/2, v/v). [**C2**] + [$CsPF_6$] = 4 mM. (a) all region and (d) enlarged region.

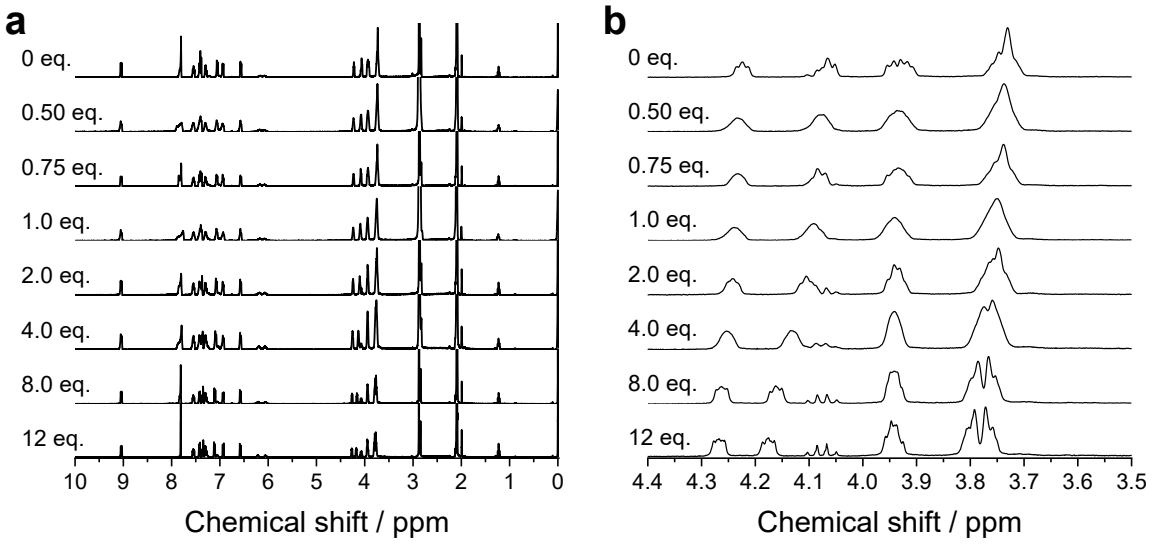

Figure S11. ^{1}H NMR spectra of **C1** with hexafluorophosphate salt of K^+ (0, 0.50, 0.75, 1.0, 2.0, 4.0, 8.0, and 12 eq.) in 2.0×10^{-3} M acetone-d_6/$CDCl_3$ (3/2, v/v) solution. (a) all region and (b) enlarged region.

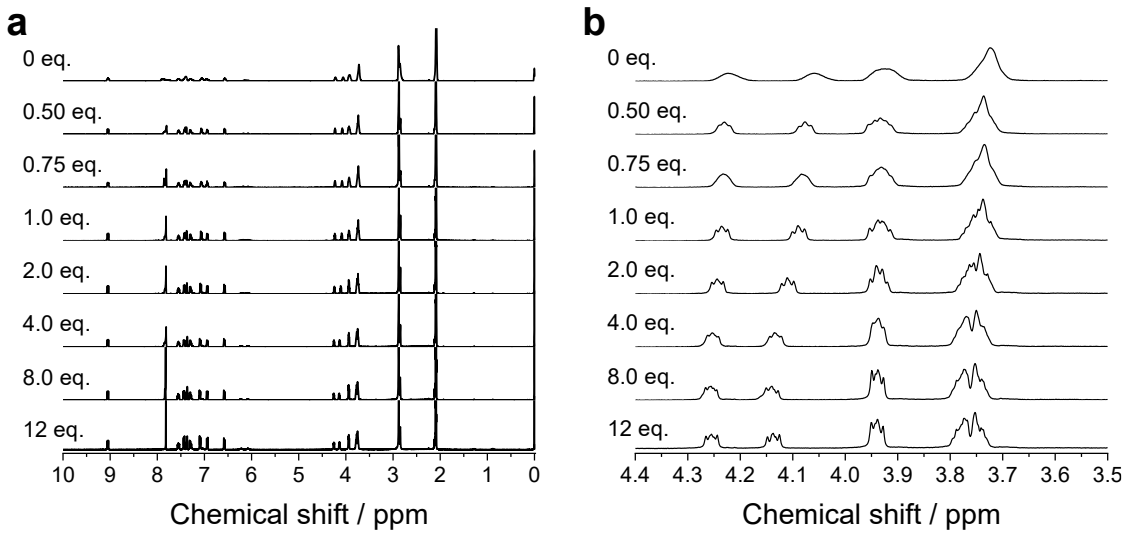

Figure S12. ^{1}H NMR spectra of **C1** with hexafluorophosphate salt of Rb^{+} (0, 0.50, 0.75, 1.0, 2.0, 4.0, 8.0, and 12 eq.) in 2.0×10^{-3} M acetone-d_6/$CDCl_3$ (3/2, v/v) solution. (a) all region and (b) enlarged region.

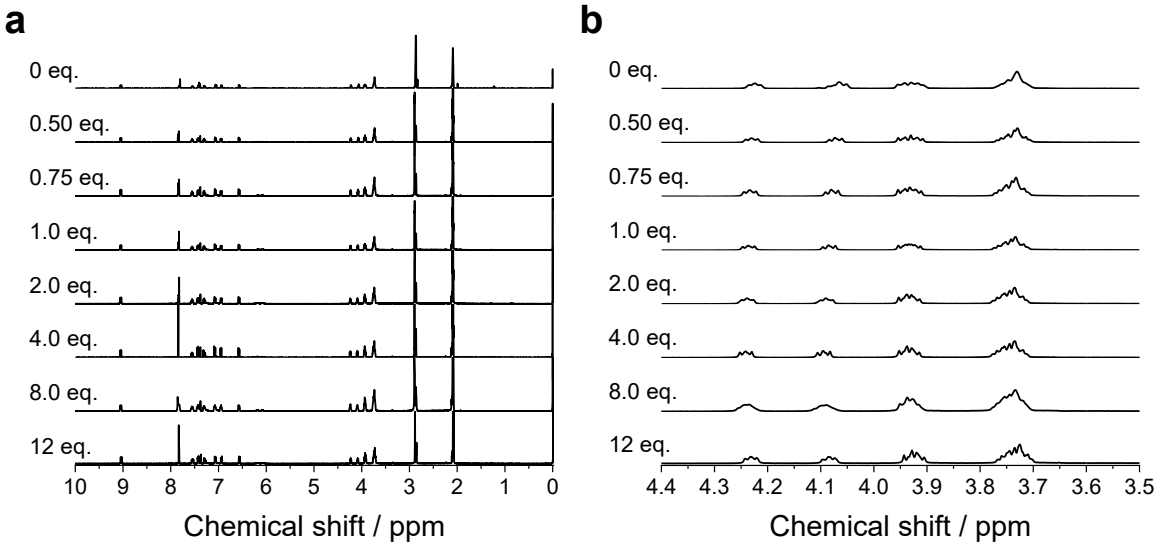

Figure S13. ^{1}H NMR spectra of **C1** with hexafluorophosphate salt of Cs^{+} (0, 0.50, 0.75, 1.0, 2.0, 4.0, 8.0, and 12 eq.) in 2.0×10^{-3} M acetone-d_6/$CDCl_3$ (3/2, v/v) solution. (a) all region and (b) enlarged region.

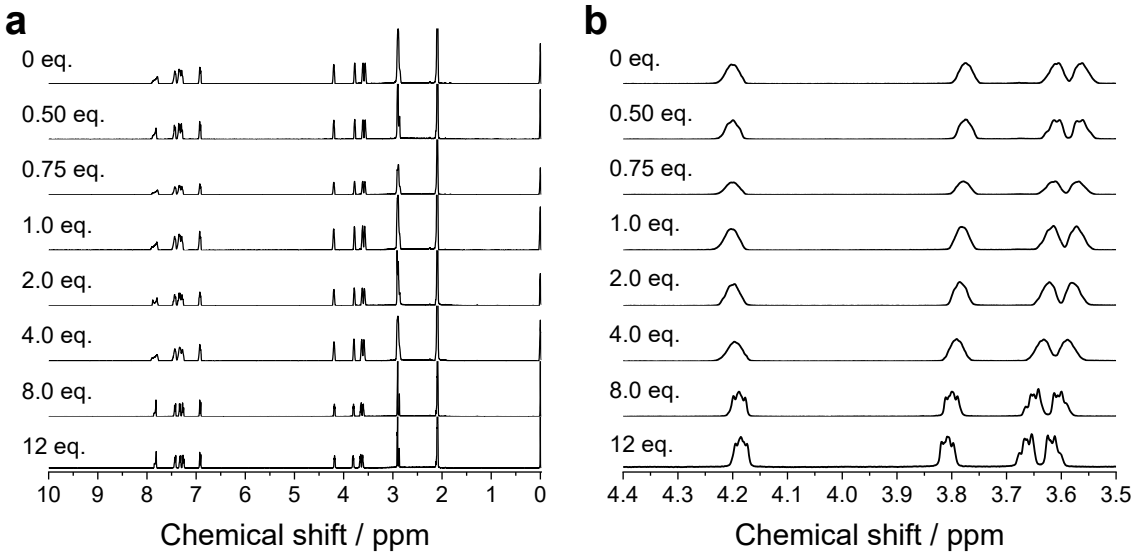

Figure S14. ^{1}H NMR spectra of **C2** with hexafluorophosphate salt of K^+ (0, 0.50, 0.75, 1.0, 2.0, 4.0, 8.0, and 12 eq.) in 2.0×10^{-3} M acetone-d_6/$CDCl_3$ (3/2, v/v) solution. (a) all region and (b) enlarged region. Note: for TEG protons around 4.2 ppm, chemical shift slightly upshifted upon cation recognition. In pseudo-crown ether systems, chemical shift of the terminal protons of the open loop slightly changes by cation recognition.[12]

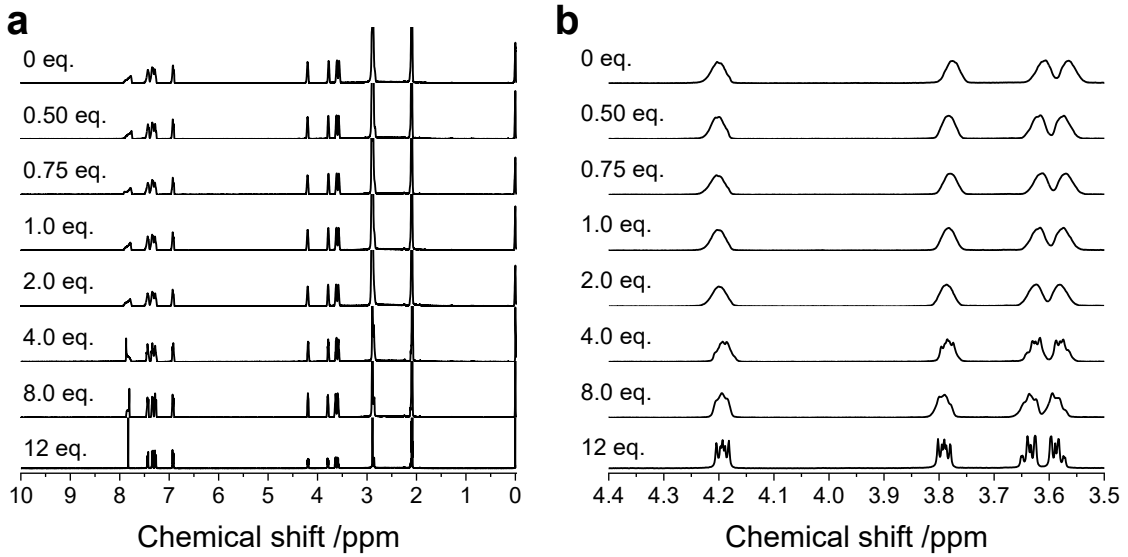

Figure S15. ^{1}H NMR spectra of **C2** with hexafluorophosphate salt of Rb^+ (0, 0.50, 0.75, 1.0, 2.0, 4.0, 8.0, and 12 eq.) in 2.0×10^{-3} M acetone-d_6/$CDCl_3$ (3/2, v/v) solution. (a) all region and (b) enlarged region. Note: for TEG protons around 4.2 ppm, chemical shift slightly upshifted upon cation recognition. In pseudo-crown ether systems, chemical shift of the terminal protons of the open loop slightly changes by cation recognition.[12]

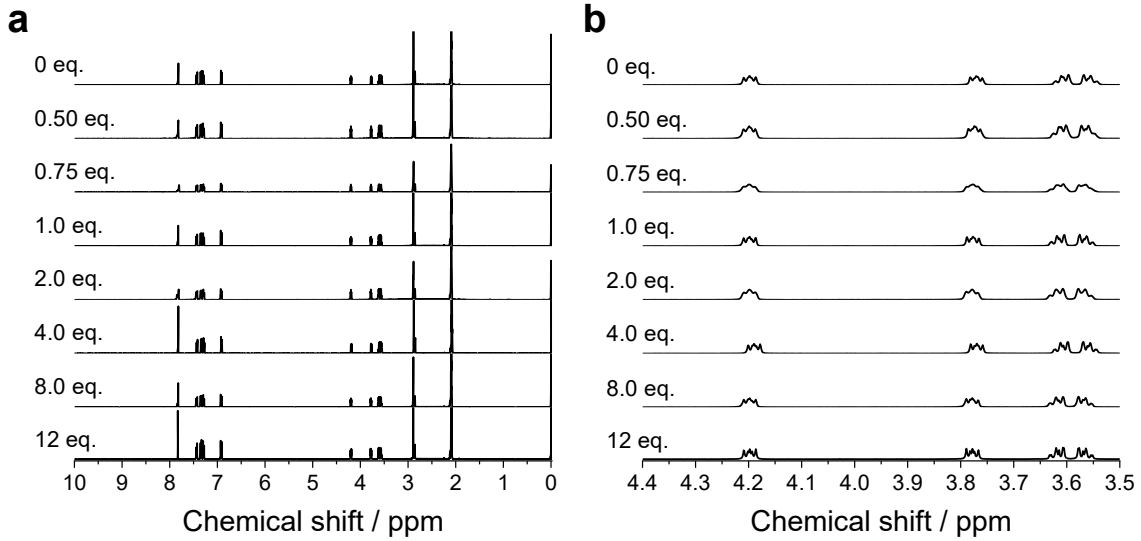

Figure S16**.** ^{1}H NMR spectra of **C2** with hexafluorophosphate salt of Cs^{+} (0, 0.50, 0.75, 1.0, 2.0, 4.0, 8.0, and 12 eq.) in 2.0×10^{-3} M acetone-d_6/$CDCl_3$ (3/2, v/v) solution**.** (a) all region and (b) enlarged region.

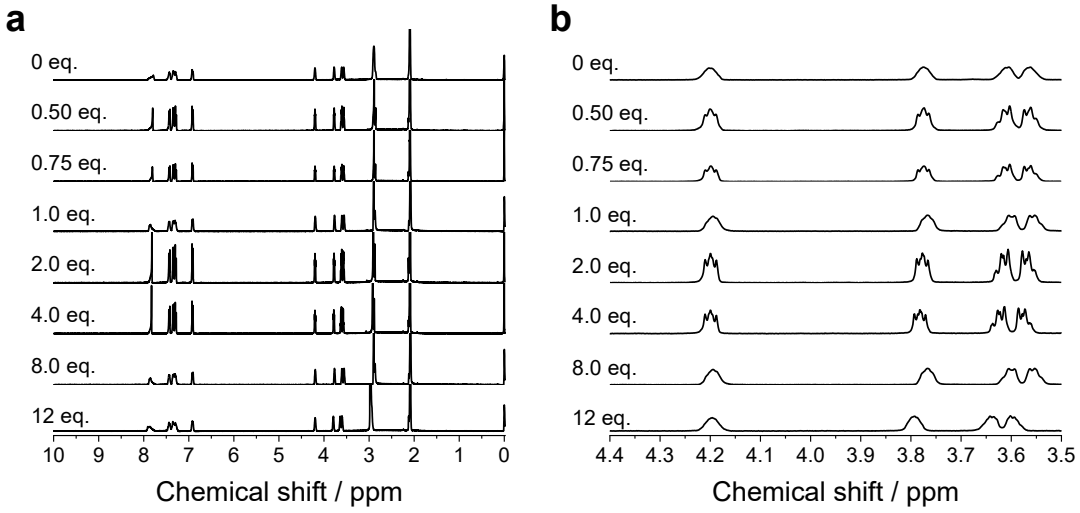

Figure S17. ^{1}H NMR spectra of **C2** with iodide salt of Na^{+} (0, 0.50, 0.75, 1.0, 2.0, 4.0, 8.0, and 12 eq.) in 2.0×10^{-3} M acetone-d_6/$CDCl_3$ (3/2, v/v) solution**.** (a) all region and (b) enlarged region.

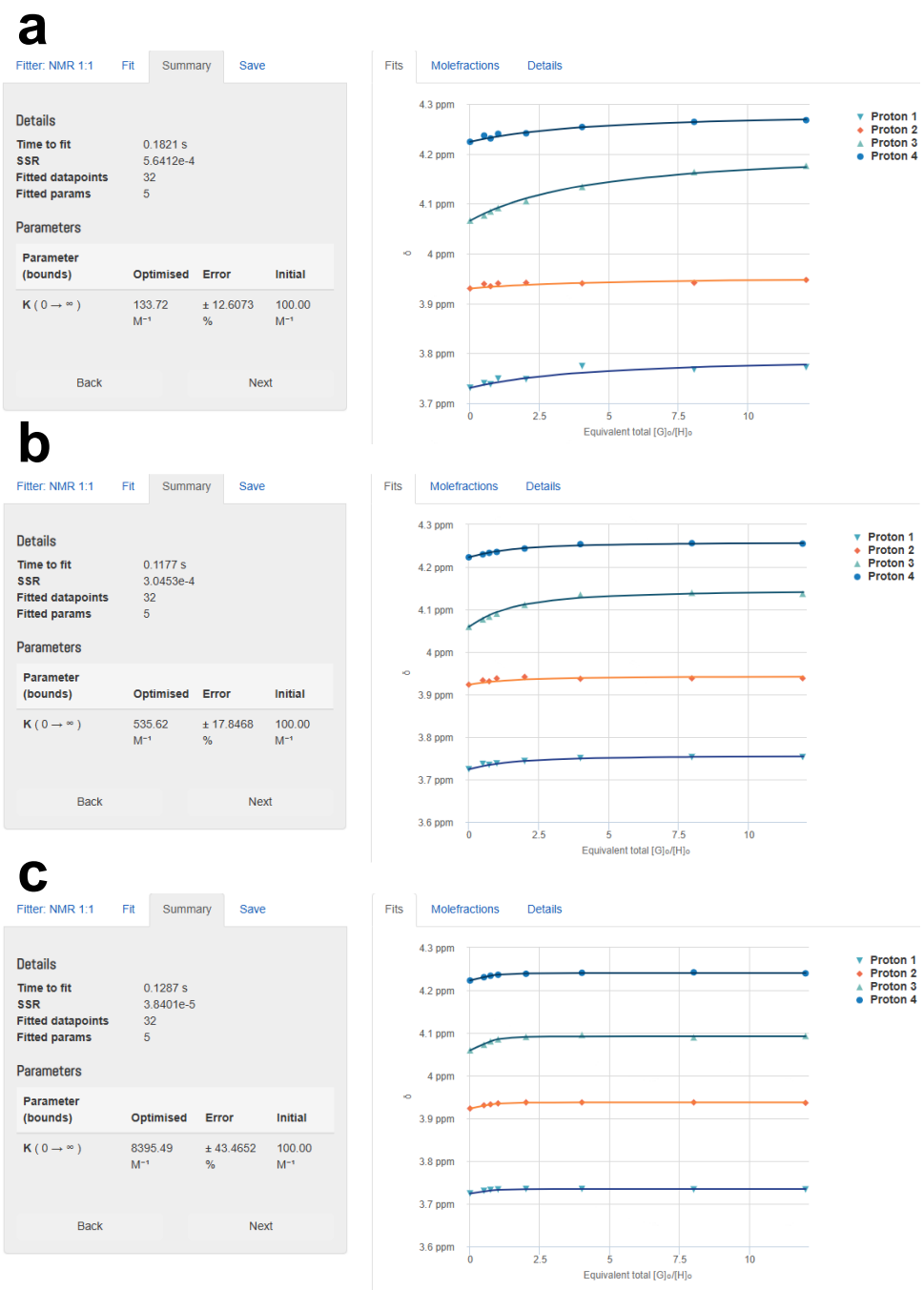

Figure S18. Curve fitting for the chemical shift change of TEG protons of **C1** with hexafluorophosphate salts of a) K^+, b) Rb^+ and c) Cs^+ measured in 2.0×10^{-3} M acetone-d_6/$CDCl_3$ (3/2, v/v) solution. Association constants were estimated by using the non-linear fitting tool provided by the open access web portal Supramolecular.org (http://supramolecular.org).

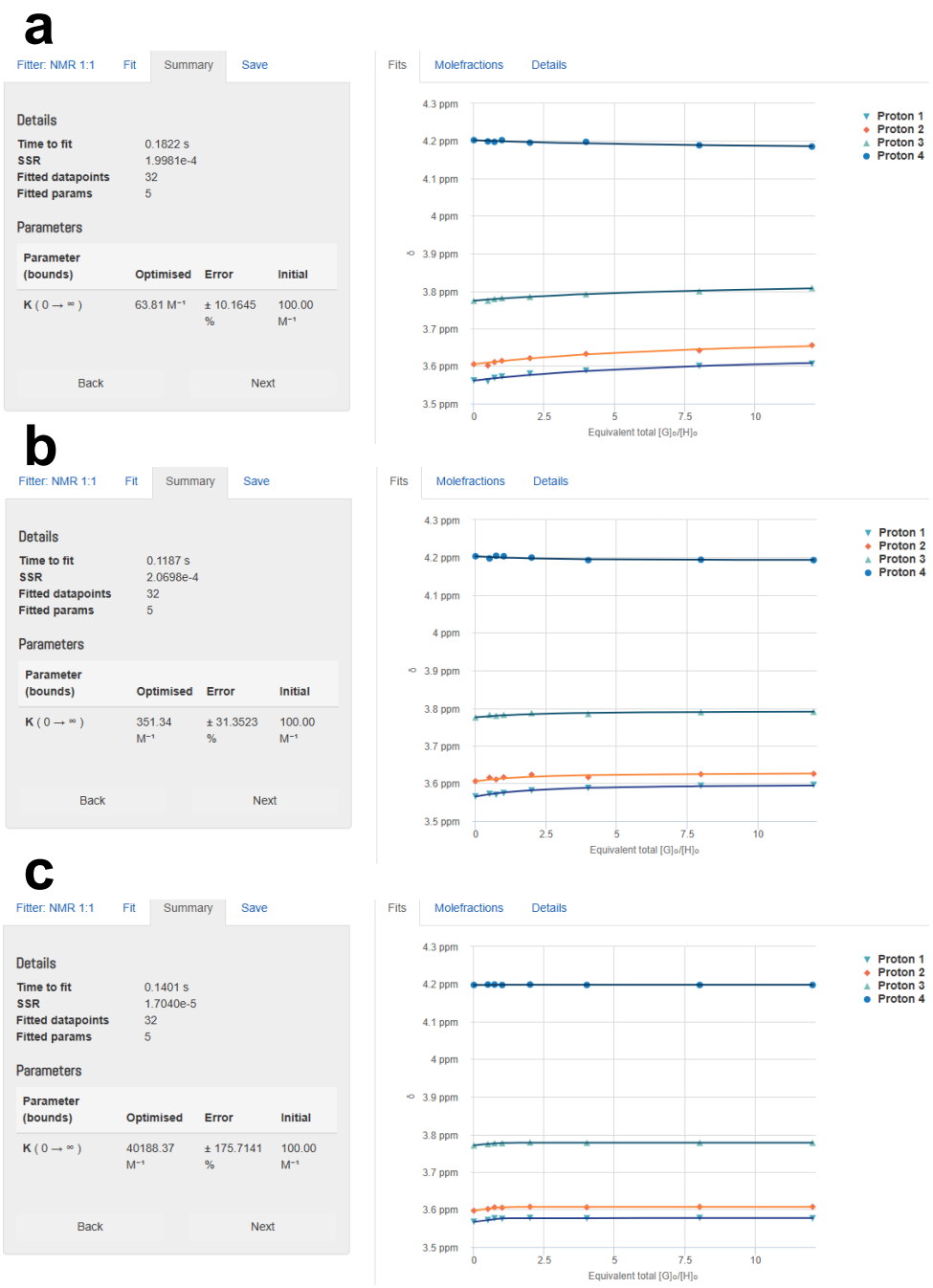

Figure S19. Curve fitting for the chemical shift change of TEG protons of **C2** with hexafluorophosphate salts of a) K^+, b) Rb^+ and c) Cs^+ measured in 2.0×10^{-3} M acetone-d_6/$CDCl_3$ (3/2, v/v) solution. Association constants were estimated by using the non-linear fitting tool provided by the open access web portal Supramolecular.org (http://supramolecular.org).

Figure S20. Curve fitting for the chemical shift change of TEG protons of **C2** with NaI measured in 2.0×10^{-3} M acetone-d_6/$CDCl_3$ (3/2, v/v) solution. Association constants were estimated by using the non-linear fitting tool provided by the open access web portal Supramolecular.org (http://supramolecular.org).

Photophysical Measurement

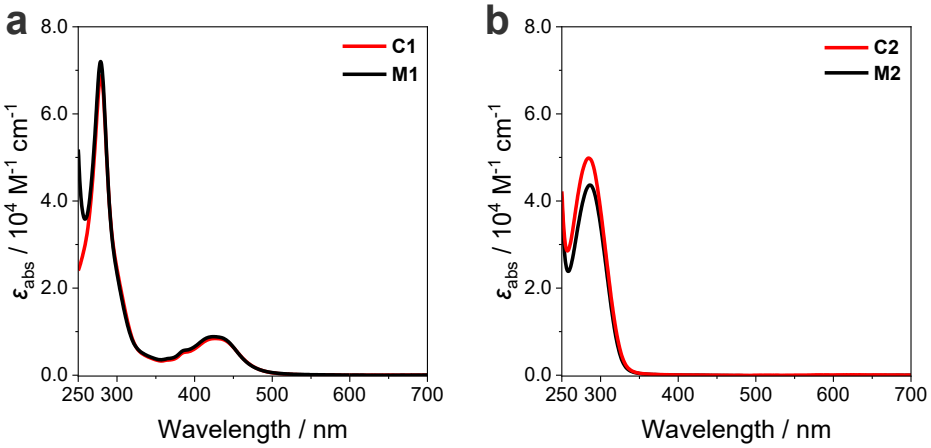

Figure S21. UV-vis absorption spectra of (a) **C1** and **M1** and (b) **C2** and **M2** in $CHCl_3$ (1.0×10^{-5} M).

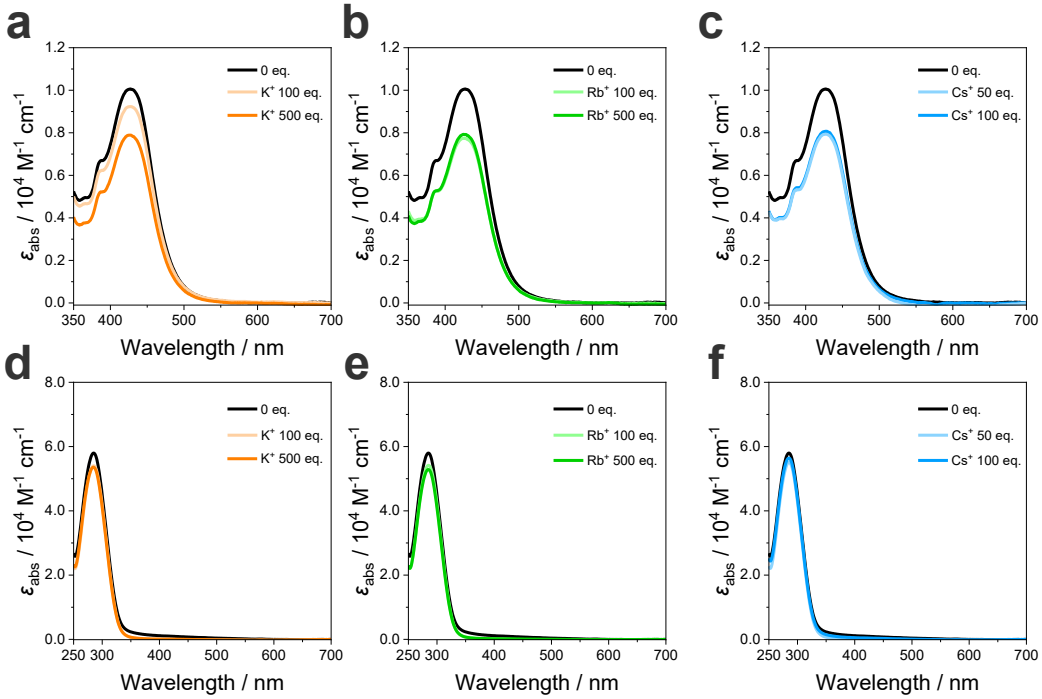

Figure S22. UV-vis absorption spectra of (a–c) **C1** in 1.0×10^{-5} M acetone/$CHCl_3$ (3/2, v/v) and (d–f) **C2** in 1.0×10^{-5} M MeCN/$CHCl_3$ (3/2, v/v) with (a, d) KPF_6, (b, e) $RbPF_6$ and (c, f) $CsPF_6$.

Table S2. Change in optical properties of **C1** and **C2** with cations

Cation [a]	Equivalents	$\lambda_{PL,max}$ / nm	
		C1 [b]	**C2** [c]
None	0	696	662
K^+	100	693	659
	500	686	650
Rb^+	100	692	662
	500	684	650
Cs^+	50	692	663
	100	688	658

[a] Hexafluorophosphate salts were used. [b] Measured in 1.0×10^{-5} M acetone/$CHCl_3$ (3/2, v/v) excited at $\lambda_{abs.max}$. [c] Measured in 1.0×10^{-5} M MeCN/$CHCl_3$ (3/2, v/v) excited at $\lambda_{abs.max}$.

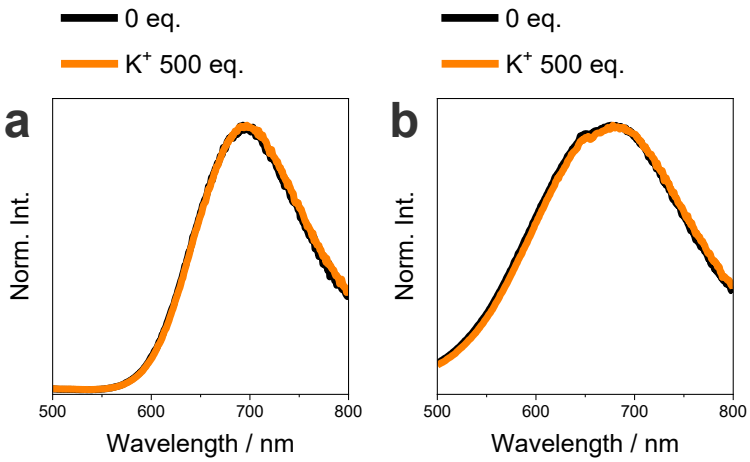

Figure S23. PL spectra of (a) **M1** in 1.0×10^{-5} M acetone/$CHCl_3$ (3/2, v/v) and (b) **M2** in 1.0×10^{-5} M MeCN/$CHCl_3$ (3/2, v/v) with KPF_6. Excited at (a) 425 nm and (b) 287 nm.

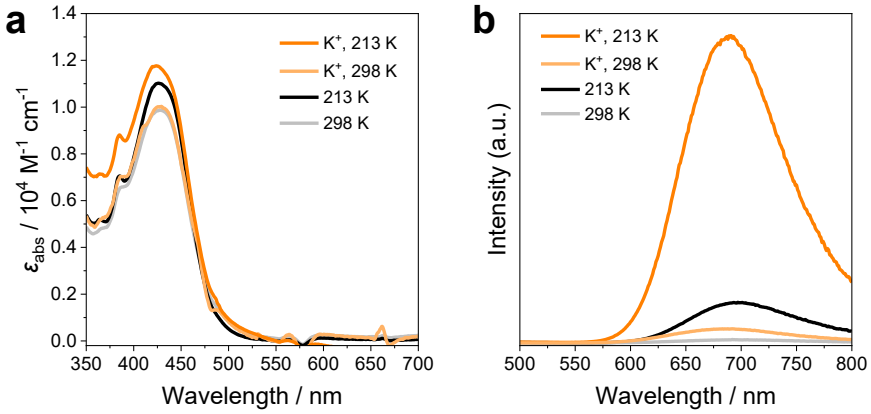

Figure S24. (a) UV-vis absorption and (b) PL spectra of **C1** in 1.0×10^{-5} M acetone/$CHCl_3$ (3/2, v/v) with 0 eq. and 500 eq. of KPF_6 at 213 K and 298 K. Excited at $\lambda_{abs.max}$.

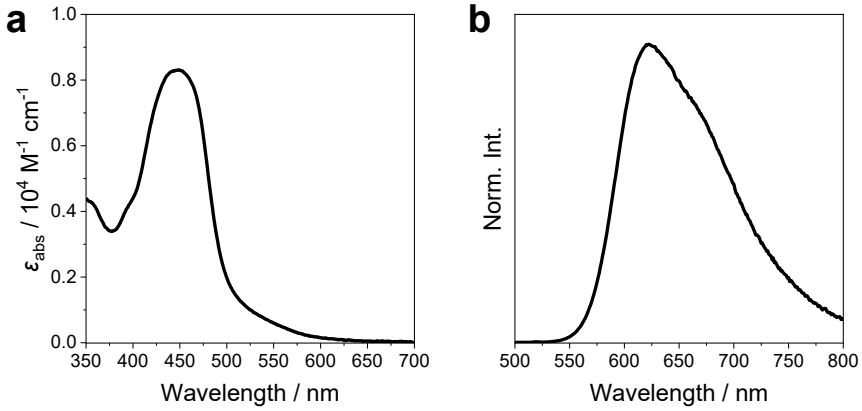

Figure S25. (a) UV-vis absorption and (b) PL spectra of $Ru(bpy)_3Cl_2{\cdot}6H_2O$ in 1.0×10^{-5} M $CHCl_3$. Excited at $\lambda_{abs.max}$.

Table S3. Optical properties of **C1** and **C1** with KPF_6 at 213 K [a]

	τ / ns [b]	τ_{ave} / ns [c]	$\Phi_{PL,rel}$ [d] (%)	k_r / 10^7 s^{-1} [e]	k_{nr} / 10^8 s^{-1} [f]
C1	1.51 (77.68%)	1.2	4.7	4.6	7.7
	0.32 (22.32%)				
C1 + 500 eq.	0.96 (8.62%)	3.2	42	13	1.8
KPF_6	3.38 (91.38%)				

[a] Measured at 213 K in 1.0×10^{-5} M acetone/$CHCl_3$ (3/2, v/v). [b] Excited at 375 nm and detected at 683 nm. [c] $\Sigma_i\tau_i f_i$, τ_i: luminescent lifetime of ith component (ns), f: relative amplitude of its component (%). [d] Relative quantum yield. [e] Radiative decay constant calculated by $\Phi_{PL,rel}/\tau_{ave}$ [f] Non-radiative decay constant calculated by $(1-\Phi_{PL,rel})/\tau_{ave}$

DFT Calculation

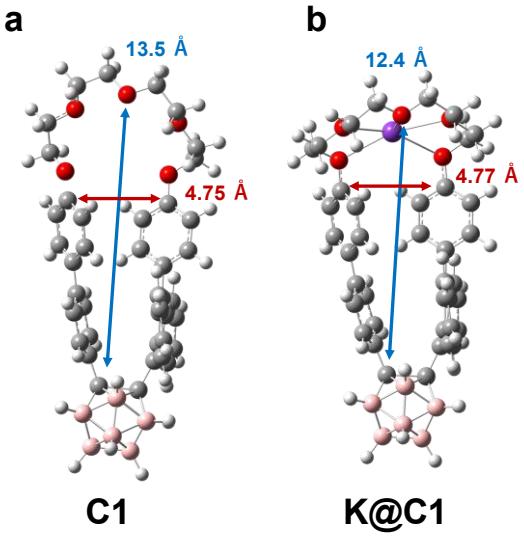

Figure S26. Optimized structures in S_0 state of (a) **C1** and (b) **K@C1**. White, hydrogen atoms; gray carbon atoms; red, oxygen atoms; pink, boron atoms; purple, potassium atom. B3PW91-D3 functional with 6-31+G(d,p) basis sets were used.

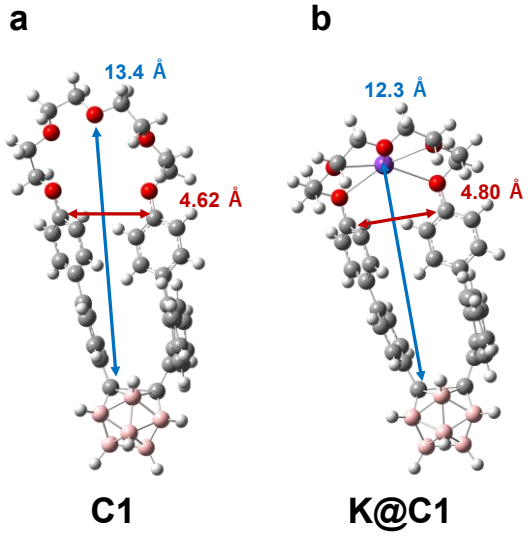

Figure S27. Optimized structures in S_1 state of (a) **C1** and (b) **K@C1**. White, hydrogen atoms; gray carbon atoms; red, oxygen atoms; pink, boron atoms; purple, potassium atom. B3PW91-D3 functional with 6-31+G(d,p) basis sets were used.

Table S4. Optimized geometry of **C1** in S_0 state

Center Number	Atomic Number	Coordinates (Angstroms)		
		x	y	z
1	5	-5.95821	0.371952	-1.15865
2	5	-6.97522	-0.82448	-0.31417
3	5	-8.21296	0.08572	0.572607
4	5	-7.97675	1.816092	0.254138
5	5	-6.58083	1.99534	-0.83851
6	5	-6.3857	2.280671	0.892258
7	5	-7.37577	1.096957	1.774304
8	5	-6.77338	-0.53959	1.41488
9	6	-5.46051	-0.38588	0.331884
10	5	-5.65241	0.824894	1.576646
11	6	-5.24466	1.380375	0.014662
12	5	-7.69656	0.627335	-1.04625
13	6	-1.34554	-1.61551	-0.0674
14	6	-1.85439	-1.27964	1.200452
15	6	-3.27796	-1.15643	1.40462
16	6	-4.15839	-1.15686	0.283172
17	6	-3.66543	-1.70994	-0.93747
18	6	-2.24595	-1.92462	-1.10693
19	6	-0.9742	-1.05485	2.305944
20	6	-1.4529	-0.88477	3.575864
21	6	-2.84933	-0.9683	3.809103
22	6	-3.7241	-1.08411	2.760956
23	6	-4.5063	-2.13147	-2.01333
24	6	-4.00378	-2.66089	-3.17334
25	6	-2.60738	-2.80855	-3.35593
26	6	-1.75995	-2.46029	-2.34024
27	6	0.117951	-1.7552	-0.2891
28	6	0.820905	-0.86931	-1.1188
29	6	2.17292	-1.03803	-1.37212
30	6	2.864324	-2.12326	-0.81674
31	6	2.18631	-3.00279	0.036852
32	6	0.826902	-2.81141	0.288987

33	6	-1.75913	2.591731	0.847373
34	6	-3.12555	2.366873	0.921837
35	6	-3.8207	1.801354	-0.15517
36	6	-3.11476	1.544573	-1.33498
37	6	-1.74628	1.775179	-1.4085
38	6	-1.03077	2.264264	-0.30656
39	6	0.439346	2.388584	-0.32976
40	6	1.19495	2.042437	0.805462
41	6	2.575681	2.136816	0.807575
42	6	3.253409	2.585639	-0.33464
43	6	2.524912	2.901531	-1.48732
44	6	1.132635	2.802937	-1.47132
45	1	-5.36895	0.145514	-2.15087
46	1	-7.1017	-1.92526	-0.73364
47	1	-9.28038	-0.40067	0.77096
48	1	-8.87189	2.599059	0.227168
49	1	-6.3541	2.836329	-1.64457
50	1	-6.02411	3.328605	1.316533
51	1	-7.81799	1.352341	2.848535
52	1	-6.73439	-1.44001	2.186929
53	1	-4.84342	0.928918	2.420738
54	1	-8.37471	0.534056	-2.01885
55	1	0.093731	-1.04893	2.117505
56	1	-0.76871	-0.72864	4.405059
57	1	-3.2323	-0.94391	4.825504
58	1	-4.77997	-1.17825	2.971579
59	1	-5.57749	-2.08787	-1.89512
60	1	-4.69038	-2.99219	-3.94749
61	1	-2.21668	-3.22815	-4.27841
62	1	-0.69198	-2.61497	-2.44643
63	1	0.295409	-0.03762	-1.57112
64	1	2.713217	-0.34222	-2.00534
65	1	2.691237	-3.84075	0.503559
66	1	0.304568	-3.50844	0.939049
67	1	-1.24596	3.024002	1.70118

68	1	-3.65242	2.614231	1.83603
69	1	-3.62205	1.113456	-2.18919
70	1	-1.22294	1.51694	-2.32484
71	1	0.687175	1.660954	1.686899
72	1	3.160397	1.860405	1.679077
73	1	3.021684	3.237892	-2.39038
74	1	0.578511	3.08335	-2.3634
75	8	4.167	-2.23892	-1.18663
76	6	4.908742	-3.37821	-0.77349
77	8	4.598457	2.691678	-0.21089
78	8	7.378704	2.104306	-0.63799
79	8	6.68524	-2.43082	0.474882
80	8	8.142576	0.010214	1.147714
81	6	5.52637	-3.21991	0.605281
82	1	4.288478	-4.28231	-0.82504
83	1	5.715873	-3.47622	-1.50439
84	6	5.360237	3.176329	-1.30548
85	6	8.530555	2.146359	0.174149
86	6	6.780327	3.363849	-0.8255
87	6	7.336164	-2.16257	1.698213
88	6	8.553523	-1.31343	1.410373
89	6	9.057488	0.744186	0.367545
90	1	5.779817	-4.21775	1.007643
91	1	4.804308	-2.75222	1.29381
92	1	4.966903	4.145029	-1.6477
93	1	5.331691	2.461937	-2.13963
94	1	9.320135	2.761045	-0.29341
95	1	8.292614	2.584211	1.157063
96	1	7.338862	3.958172	-1.56969
97	1	6.757212	3.935245	0.1163
98	1	7.651906	-3.1035	2.182455
99	1	6.668096	-1.62595	2.390574
100	1	9.241268	-1.34	2.272831
101	1	9.077788	-1.74459	0.543257
102	1	10.0423	0.806509	0.863865

103	1	9.198332	0.265316	-0.61481

Table S5. Optimized geometry of **K@C1** in S_0 state

Center Number	Atomic Number	Coordinates (Angstroms)		
		x	y	z
1	5	6.157217	-0.33872	-0.89747
2	5	7.095709	0.758764	0.14398
3	5	8.21037	-0.25138	1.08623
4	5	7.972173	-1.94628	0.610927
5	5	6.699283	-1.99918	-0.63421
6	5	6.31223	-2.40696	1.039132
7	5	7.227403	-1.32567	2.111733
8	5	6.702506	0.350108	1.815956
9	6	5.510579	0.308525	0.589029
10	5	5.540924	-0.98986	1.758974
11	6	5.294552	-1.3977	0.120899
12	5	7.863826	-0.65522	-0.61642
13	6	1.495949	1.737823	-0.08067
14	6	1.873974	1.317877	1.206681
15	6	3.267595	1.104945	1.518528
16	6	4.238212	1.129309	0.475187
17	6	3.878641	1.777513	-0.74396
18	6	2.487276	2.053808	-1.02644
19	6	0.894549	1.09642	2.226912
20	6	1.256398	0.835254	3.519691
21	6	2.631039	0.813125	3.86724
22	6	3.593538	0.928256	2.899818
23	6	4.827235	2.23351	-1.71132
24	6	4.447619	2.834112	-2.88278
25	6	3.077067	3.021391	-3.18943
26	6	2.129633	2.652406	-2.27494
27	6	0.057617	1.941885	-0.40624
28	6	-0.63364	1.056664	-1.24172
29	6	-1.98233	1.237324	-1.52373

30	6	-2.67199	2.321115	-0.97333
31	6	-1.99575	3.233467	-0.1601
32	6	-0.64147	3.034974	0.113584
33	6	1.746887	-2.69069	0.432633
34	6	3.092293	-2.46188	0.686271
35	6	3.890931	-1.77731	-0.23863
36	6	3.318406	-1.39111	-1.45399
37	6	1.972505	-1.62357	-1.70886
38	6	1.155282	-2.24873	-0.75836
39	6	-0.29987	-2.37335	-0.98417
40	6	-1.20071	-2.10386	0.056934
41	6	-2.57541	-2.12251	-0.16213
42	6	-3.06614	-2.40916	-1.43613
43	6	-2.19126	-2.69299	-2.48287
44	6	-0.81852	-2.677	-2.25283
45	1	5.67971	-0.02529	-1.9253
46	1	7.279078	1.885867	-0.17133
47	1	9.257963	0.188007	1.435315
48	1	8.844432	-2.7533	0.6178
49	1	6.53209	-2.7705	-1.51999
50	1	5.87882	-3.47195	1.332814
51	1	7.544183	-1.67311	3.203262
52	1	6.600503	1.19611	2.640903
53	1	4.632531	-1.13172	2.490729
54	1	8.643476	-0.51048	-1.50142
55	1	-0.1542	1.173393	1.960816
56	1	0.499045	0.688981	4.284662
57	1	2.926659	0.711597	4.907323
58	1	4.630989	0.944517	3.200171
59	1	5.881049	2.159491	-1.49307
60	1	5.209789	3.189752	-3.56996
61	1	2.786094	3.489939	-4.12493
62	1	1.080401	2.842061	-2.47454
63	1	-0.10653	0.215487	-1.6749
64	1	-2.49827	0.545544	-2.18331

65	1	-2.491	4.098748	0.264626
66	1	-0.11958	3.743716	0.750202
67	1	1.150258	-3.22075	1.169508
68	1	3.52027	-2.80491	1.620893
69	1	3.910986	-0.86566	-2.1921
70	1	1.549018	-1.26498	-2.6431
71	1	-0.81804	-1.82386	1.033997
72	1	-3.26302	-1.88358	0.644687
73	1	-2.59319	-2.91482	-3.46691
74	1	-0.13897	-2.90825	-3.06794
75	8	-4.01478	2.39444	-1.28772
76	19	-5.60347	0.038878	-0.81668
77	6	-4.76137	3.555133	-0.92386
78	8	-4.42754	-2.32668	-1.70083
79	8	-6.39622	-2.5084	0.295466
80	8	-6.17433	2.406303	0.623785
81	8	-6.91496	-0.11295	1.700515
82	6	-5.27428	3.501374	0.501798
83	1	-4.17208	4.465297	-1.085
84	1	-5.60865	3.57998	-1.61565
85	6	-5.19254	-3.52328	-1.48455
86	6	-6.8279	-2.499	1.648668
87	6	-5.63376	-3.65991	-0.04326
88	6	-6.66103	2.247156	1.951321
89	6	-7.62117	1.083953	2.001414
90	6	-7.69738	-1.28716	1.881116
91	1	-5.78925	4.447405	0.729905
92	1	-4.44523	3.380878	1.213165
93	1	-4.61308	-4.40334	-1.78794
94	1	-6.06644	-3.43595	-2.13679
95	1	-7.4134	-3.40316	1.873307
96	1	-5.9595	-2.47291	2.324519
97	1	-6.24101	-4.57207	0.062894
98	1	-4.76262	-3.75237	0.621955
99	1	-7.1875	3.157051	2.276244

100	1	-5.82304	2.065869	2.641048
101	1	-8.05339	1.030869	3.011877
102	1	-8.44395	1.235858	1.285603
103	1	-8.09486	-1.32775	2.90627
104	1	-8.54795	-1.29276	1.182188

Table S6. Optimized geometry of **C1** in S_1 state

Center Number	Atomic Number	Coordinates (Angstroms)		
		x	y	z
1	5	-5.73664	0.85819	-1.00967
2	5	-7.06194	-0.29447	-0.53996
3	5	-8.16064	0.658856	0.487019
4	5	-7.64735	2.346902	0.505531
5	5	-6.19136	2.536334	-0.51658
6	5	-6.0365	2.467278	1.269199
7	5	-7.20327	1.271725	1.865286
8	5	-6.90596	-0.36246	1.239708
9	6	-5.60447	-0.39986	0.224344
10	5	-5.51955	0.7589	1.554146
11	6	-4.97044	1.750806	0.250199
12	5	-7.44878	1.379533	-0.98705
13	6	-1.65038	-1.78124	-0.24124
14	6	-2.23089	-1.78122	1.05706
15	6	-3.65717	-1.67008	1.215578
16	6	-4.46201	-1.29962	0.07688
17	6	-3.92822	-1.63339	-1.22219
18	6	-2.51414	-1.83265	-1.37684
19	6	-1.43817	-1.83543	2.232267
20	6	-2.00682	-1.97275	3.48888
21	6	-3.4004	-2.03256	3.621868
22	6	-4.20335	-1.85291	2.502728
23	6	-4.75145	-1.78346	-2.35818
24	6	-4.23147	-2.08434	-3.60999
25	6	-2.85008	-2.24773	-3.76768

26	6	-2.01336	-2.13437	-2.66843
27	6	-0.1937	-1.83603	-0.4328
28	6	0.461536	-0.8535	-1.20319
29	6	1.825292	-0.89873	-1.42524
30	6	2.585374	-1.96833	-0.92471
31	6	1.95912	-2.9504	-0.14087
32	6	0.590765	-2.87253	0.100361
33	6	-1.36476	2.189382	1.256186
34	6	-2.7416	2.07476	1.328004
35	6	-3.52947	1.979702	0.163577
36	6	-2.86326	2.04569	-1.07603
37	6	-1.48483	2.17277	-1.14404
38	6	-0.69243	2.223544	0.018557
39	6	0.774952	2.293351	-0.04374
40	6	1.570159	1.700544	0.959008
41	6	2.949578	1.783701	0.933194
42	6	3.5967	2.467071	-0.10787
43	6	2.833722	3.021091	-1.14335
44	6	1.442901	2.933915	-1.09718
45	1	-5.14074	0.698503	-2.01864
46	1	-7.40548	-1.20819	-1.21778
47	1	-9.30659	0.34543	0.57185
48	1	-8.42827	3.240202	0.607604
49	1	-5.88564	3.463548	-1.1964
50	1	-5.61286	3.342027	1.955608
51	1	-7.65086	1.390275	2.96235
52	1	-7.11853	-1.32975	1.898012
53	1	-4.75702	0.539916	2.429507
54	1	-8.07951	1.571766	-1.97856
55	1	-0.36015	-1.76032	2.140367
56	1	-1.36861	-2.03453	4.365867
57	1	-3.85718	-2.17779	4.595981
58	1	-5.27947	-1.84695	2.618662
59	1	-5.82182	-1.67967	-2.24545
60	1	-4.90138	-2.19684	-4.45707

61	1	-2.43174	-2.48389	-4.74193
62	1	-0.94955	-2.30392	-2.79243
63	1	-0.12193	-0.0343	-1.60725
64	1	2.32842	-0.11874	-1.98766
65	1	2.51793	-3.78214	0.272822
66	1	0.110509	-3.65598	0.679863
67	1	-0.79743	2.277545	2.178005
68	1	-3.22399	2.054292	2.298696
69	1	-3.43768	1.974986	-1.99277
70	1	-1.01107	2.190334	-2.12213
71	1	1.093111	1.137089	1.7554
72	1	3.559239	1.322084	1.703261
73	1	3.304509	3.540499	-1.97041
74	1	0.868733	3.414224	-1.88445
75	8	3.893648	-1.97012	-1.27149
76	6	4.677637	-3.13432	-1.02656
77	8	4.942522	2.54846	-0.00252
78	8	7.697721	2.067692	-0.51522
79	8	6.52594	-2.40488	0.264213
80	8	8.250705	-0.21196	1.102182
81	6	5.330532	-3.1431	0.346317
82	1	4.073617	-4.03617	-1.18403
83	1	5.46714	-3.1127	-1.78218
84	6	5.682377	3.234718	-1.00076
85	6	8.825449	1.95743	0.324194
86	6	7.107525	3.344465	-0.5114
87	6	7.239898	-2.33372	1.48079
88	6	8.530742	-1.58723	1.231475
89	6	9.240747	0.507401	0.403499
90	1	5.541234	-4.18686	0.642582
91	1	4.645718	-2.71255	1.094918
92	1	5.278843	4.24633	-1.15373
93	1	5.642395	2.684025	-1.95041
94	1	9.669097	2.553626	-0.06546
95	1	8.588444	2.319565	1.337395

96	1	7.662107	4.040842	-1.16401
97	1	7.094387	3.769661	0.504761
98	1	7.471697	-3.34771	1.851197
99	1	6.652167	-1.81073	2.251806
100	1	9.230524	-1.76423	2.066282
101	1	8.989055	-1.98588	0.312705
102	1	10.21513	0.446698	0.919785
103	1	9.366112	0.10388	-0.61414

Table S7. Optimized geometry of **K@C1** in S_1 state

Center Number	Atomic Number	Coordinates (Angstroms)		
		x	y	z
1	5	5.980312	-0.70342	-0.79031
2	5	7.169889	0.474309	-0.08612
3	5	8.194396	-0.49679	1.001953
4	5	7.773651	-2.20378	0.847917
5	5	6.46453	-2.38651	-0.35923
6	5	6.088877	-2.45015	1.395611
7	5	7.11197	-1.2525	2.210978
8	5	6.807238	0.406331	1.660604
9	6	5.627579	0.432101	0.501231
10	5	5.44936	-0.79496	1.732502
11	6	5.113908	-1.72337	0.298049
12	5	7.704337	-1.14361	-0.59142
13	6	1.688452	1.847444	-0.25206
14	6	2.151693	1.790561	1.087897
15	6	3.55364	1.618135	1.365609
16	6	4.457877	1.307505	0.289009
17	6	4.038253	1.694988	-1.03203
18	6	2.642256	1.904299	-1.30439
19	6	1.257361	1.870223	2.18664
20	6	1.711993	1.939662	3.494721
21	6	3.086905	1.909002	3.754527
22	6	3.981563	1.725059	2.70679

23	6	4.956494	1.894177	-2.08706
24	6	4.543069	2.231519	-3.37117
25	6	3.179379	2.372438	-3.64881
26	6	2.250183	2.218847	-2.62946
27	6	0.244191	1.964279	-0.54872
28	6	-0.43153	0.94177	-1.23472
29	6	-1.79013	1.033443	-1.50868
30	6	-2.50622	2.169575	-1.11854
31	6	-1.85186	3.207352	-0.44831
32	6	-0.49097	3.093784	-0.16725
33	6	1.479628	-2.55197	0.85107
34	6	2.832626	-2.36826	1.078692
35	6	3.708112	-2.01178	0.030995
36	6	3.158309	-1.87779	-1.25812
37	6	1.803682	-2.06269	-1.482
38	6	0.925083	-2.38851	-0.43297
39	6	-0.52295	-2.50018	-0.67081
40	6	-1.44983	-2.10088	0.308591
41	6	-2.81885	-2.13638	0.065192
42	6	-3.2907	-2.56673	-1.17695
43	6	-2.39544	-2.97972	-2.16204
44	6	-1.02899	-2.95143	-1.90506
45	1	5.511147	-0.50297	-1.85662
46	1	7.520032	1.453273	-0.66181
47	1	9.301048	-0.13644	1.247585
48	1	8.579577	-3.06742	0.986933
49	1	6.288034	-3.26763	-1.13742
50	1	5.633019	-3.38694	1.96925
51	1	7.427949	-1.43347	3.343409
52	1	6.888175	1.33611	2.396156
53	1	4.562259	-0.68081	2.506881
54	1	8.453906	-1.2346	-1.51036
55	1	0.190255	1.877987	1.992825
56	1	1.00101	2.021741	4.31159
57	1	3.46021	1.998042	4.769793

58	1	5.039557	1.673581	2.924417
59	1	6.015275	1.809173	-1.88463
60	1	5.283798	2.38385	-4.14977
61	1	2.845942	2.623216	-4.65134
62	1	1.196616	2.364182	-2.84332
63	1	0.119073	0.058685	-1.53895
64	1	-2.29565	0.2266	-2.03178
65	1	-2.37032	4.109497	-0.14538
66	1	0.013493	3.907264	0.346361
67	1	0.844165	-2.85147	1.680011
68	1	3.23012	-2.50608	2.078487
69	1	3.799942	-1.60079	-2.08604
70	1	1.418876	-1.91097	-2.48721
71	1	-1.09214	-1.71113	1.256559
72	1	-3.51812	-1.80419	0.828462
73	1	-2.77861	-3.3181	-3.12016
74	1	-0.34274	-3.29956	-2.67093
75	8	-3.84822	2.174454	-1.43784
76	19	-5.64918	-0.00929	-0.8338
77	6	-4.59773	3.381705	-1.29201
78	8	-4.64602	-2.50431	-1.48003
79	8	-6.56947	-2.38157	0.551487
80	8	-6.09757	2.513417	0.34862
81	8	-6.96479	0.174945	1.689448
82	6	-5.1597	3.554104	0.104943
83	1	-3.99511	4.251809	-1.57596
84	1	-5.42084	3.301374	-2.00885
85	6	-5.43757	-3.64484	-1.11374
86	6	-6.98874	-2.20461	1.896496
87	6	-5.86516	-3.59875	0.337774
88	6	-6.60539	2.534042	1.677919
89	6	-7.61743	1.427551	1.848245
90	6	-7.79964	-0.93549	1.99698
91	1	-5.65131	4.536751	0.175244
92	1	-4.35708	3.515613	0.854998

93	1	-4.88486	-4.57042	-1.31498
94	1	-6.31636	-3.61079	-1.76423
95	1	-7.61369	-3.05018	2.220978
96	1	-6.11477	-2.14574	2.563173
97	1	-6.51225	-4.46374	0.549911
98	1	-4.9913	-3.65735	1.002972
99	1	-7.09372	3.497994	1.885012
100	1	-5.78327	2.398877	2.396557
101	1	-8.0565	1.508013	2.853995
102	1	-8.42941	1.535032	1.112221
103	1	-8.19293	-0.84543	3.020577
104	1	-8.653	-0.97726	1.302764

Table S8. Result of TD-DFT calculation for **C1** in the S_0 geometry

Excited State	Energy / eV	Wavelength / nm	*f*	Composition	Coefficient
1	2.7382	452.8	0.1602		
				HOMO -> LUMO	0.69969
2	3.0283	409.42	0.0045		
				HOMO-1 -> LUMO	0.70383
3	3.2518	381.27	0.0027		
				HOMO-2 -> LUMO	0.70107
4	3.4945	354.8	0.0026		
				HOMO -> LUMO+1	0.70356
5	3.5779	346.53	0.0089		
				HOMO-3 -> LUMO	0.54574
				HOMO -> LUMO+2	-0.41485

Table S9. Result of TD-DFT calculation for **K@C1** in the S_0 geometry

Excited State	Energy / eV	Wavelength / nm	*f*	Composition	Coefficient
1	2.7978	443.15	0.136		
				HOMO -> LUMO	0.70155

2	3.2082	386.46	0.0001		
				HOMO -> LUMO+1	0.70337
3	3.4959	354.65	0.0013		
				HOMO-1 -> LUMO	0.31778
				HOMO -> LUMO+2	0.57762
				HOMO -> LUMO+3	-0.20929
4	3.652	339.5	0.014		
				HOMO-1 -> LUMO	0.44883
				HOMO -> LUMO+2	-0.38976
				HOMO -> LUMO+3	-0.17368
				HOMO -> LUMO+5	0.14411
				HOMO -> LUMO+6	0.24395
				HOMO -> LUMO+9	0.15323
5	3.8089	325.51	0.005		
				HOMO-2 -> LUMO	0.70388

Table S10. Result of TD-DFT calculation for **C1** in the S_1 geometry

Excited State	Energy / eV	Wavelength / nm	*f*	Composition	Coefficient
1	1.9592	632.83	0.1536		
				HOMO -> LUMO	0.70073
2	2.4476	506.56	0.1809		
				HOMO-1 -> LUMO	-0.69417
3	2.8122	440.88	0.0242		
				HOMO-2 -> LUMO	-0.70276
4	2.9783	416.30	0.0913		
				HOMO -> LUMO+1	-0.69448
5	3.1665	391.55	0.0100		
				HOMO-3 -> LUMO	0.31083
				HOMO-2 -> LUMO	0.60660
				HOMO -> LUMO+2	-0.11334

Table S11. Result of TD-DFT calculation for **K@C1** in the S_1 geometry

Excited State	Energy / eV	Wavelength / nm	*f*	Composition	Coefficient
1	2.0453	606.20	0.1536		
				HOMO -> LUMO	-0.70292
2	2.8506	434.94	0.1809		
				HOMO-1 -> LUMO	-0.12284
				HOMO -> LUMO+1	-0.69068
3	3.1476	393.90	0.0242		
				HOMO-3 -> LUMO	0.20501
				HOMO-2 -> LUMO	0.60474
				HOMO-1 -> LUMO	0.24450

Reference

1 D. F. Eaton, *Pure and Appl. Chem.*, 1988, **60**, 1107–1114.

2 G. M. Sheldrick, *Acta Crystallogr. A*, 2015, **71**, 3–8.

3 G. M. Sheldrick, *Acta Crystallogr. C Struct. Chem*, 2015, **71**, 3–8.

4 O. V. Dolomanov, L. J. Bourhis, R. J. Gildea, J. A. K. Howard and H. Puschmann, *J Appl. Crystallogr*, 2009, **42**, 339–341.

5 C. F. Macrae, I. J. Bruno, J. A. Chisholm, P. R. Edgington, P. McCabe, E. Pidcock, L. Rodriguez-Monge, R. Taylor, J. Van De Streek and P. A. Wood, *J. Appl. Crystallogr.*, 2008, **41**, 466–470.

6 M. J.Frisch, G. W.Trucks, H. B.Schlegel, G. E.Scuseria, M. A.Robb, J. R.Cheeseman, G.Scalmani, V.Barone, G. A.Petersson, H.Nakatsuji, X.Li, M.Caricato, A. V.Marenich, J.Bloino, B. G.Janesko, R.Gomperts, B.Mennucci, H. P.Hratchian, J. V.Ortiz, A. F.Izmaylov, J. L.Sonnenberg, D.Williams-Young, F.Ding, F.Lipparini, F.Egidi, J.Goings, B.Peng, A.Petrone, T.Henderson, D.Ranasinghe, V. G.Zakrzewski, J.Gao, N.Rega, G.Zheng, W.Liang, M.Hada, M.Ehara, K.Toyota, R.Fukuda, J.Hasegawa, M.Ishida, T.Nakajima, Y.Honda, O.Kitao, H.Nakai, T.Vreven, K.Throssell, J. A.Montgomery Jr, J. E.Peralta, F.Ogliaro, M. J.Bearpark, J. J.Heyd, E. N.Brothers, K. N.Kudin, V. N.Staroverov, T. A.Keith, R.Kobayashi, J.Normand, K.Raghavachari, A. P.Rendell, J. C.Burant, S. S.Iyengar, J.Tomasi, M.Cossi, J. M.Millam, M.Klene, C.Adamo, R.Cammi, J. W.Ochterski, R. L.Martin, K.Morokuma, O.Farkas, J. B.Foresman and D. J.Fox, Gaussian 16, Rev. C.01, Gaussian, Inc., Wallingford CT.

7 K. Yuhara and K. Tanaka, *Chem. Sci.*, 2025, **16**, 6495−6506.

8 X. Yang, H. Li, D. Shao and G. He, *Chem. Commun.*, 2023, **59**, 7643–7646.

9 Y. Chen, L. Wang, X. Pan, J. Wu, W. Zhang, Z. Zhang and X. Zhu, *Polym. Chem.*, 2018, **9**, 2438–2445.

10 B. Fuchs, A. Nelson, A. Star, J. F. Stoddart and S. Vidal, *Angew. Chem. Int. Ed.,* 2003, **42**, 4220–4224.

11 X. Li, J. Y. C. Lim and P. D. Beer, *Chem. Eur. J.*, 2018, **24**, 17788–17795.

12 T. Terashima, M. Kawabe, Y. Miyabara, H. Yoda, M. Sawamoto, *Nat. Commun.*, 2013, **4**, 2321.